RESEARCH ARTICLE

Mutations in TIC100 impair and repair chloroplast protein import and impact retrograde signalling

Naresh Loudya[1,2], Douglas P. F. Maffei[1,†], Jocelyn Bédard[2], Sabri Mohd. Ali[2], Paul Devlin[1], R. Paul Jarvis[2] and Enrique López-Juez[1]

[a]Department of Biological Sciences, Royal Holloway University of London, Egham, Surrey TW20 0EX, UK

[b]Department of Plant Sciences, University of Oxford, South Parks Road, Oxford, OX1 3RB, UK

[†]Present address: Seagen, 21717 30th Drive S.E., Bothell, WA 98021, USA

Corresponding authors: Enrique López-Juez. E-mail: e.lopez@rhul.ac.uk and R. Paul Jarvis. E-mail: paul.jarvis@plants.ox.ac.uk

Short title: TIC100 in chloroplast protein import

One sentence summary: Complementary mutations in TIC100 of the chloroplast inner envelope membrane cause reductions or corrective improvements in chloroplast protein import, and highlight a signalling role.

The author responsible for distribution of materials integral to the findings presented in this article in accordance with the policy described in the Instructions for Authors (www.plantcell.org) is: Enrique López-Juez (e.lopez@rhul.ac.uk).

Abstract

Chloroplast biogenesis requires synthesis of proteins in the nucleocytoplasm and the chloroplast itself. Nucleus-encoded chloroplast proteins are imported via multiprotein translocons in the organelle's envelope membranes. Controversy exists around whether a 1 MDa complex comprising TIC20, TIC100 and other proteins constitutes the inner membrane TIC translocon. The Arabidopsis *cue8* virescent mutant is broadly defective in plastid development. We identify *CUE8* as *TIC100*. The *tic100^{cue8}* mutant accumulates reduced levels of 1 MDa complex components and exhibits reduced import of two nucleus-encoded chloroplast proteins of different import profiles. A search for suppressors of *tic100^{cue8}* identified a second mutation within the same gene, *tic100^{soh1}*, which rescues the visible, 1 MDa complex-subunit abundance, and chloroplast protein import phenotypes. *tic100^{soh1}* retains but rapidly exits virescence, and rescues the synthetic lethality of *tic100^{cue8}* when retrograde signalling is impaired by the *gun1* mutation. Alongside the strong virescence, changes in RNA editing and the presence of unimported precursor proteins show that a strong signalling response is triggered when TIC100 function is altered. Our results are consistent with a role for TIC100, and by extension the 1 MDa complex, in the chloroplast import of photosynthetic and non-photosynthetic proteins, a process which initiates retrograde signalling.

40   **Introduction**

41   Chloroplast-containing photosynthetic eukaryotes sustain the biosphere.

42   Chloroplast biogenesis is a complex process which in plants requires the

43   involvement of 2000-3000 nucleus-encoded proteins and approximately 80

44   proteins encoded by the chloroplast's own genome (Jarvis and López-Juez,

45   2013). The majority of proteins (those which are nucleus-encoded) need to be

46   imported into the chloroplasts through the double-membrane envelope. This is

47   achieved by the operation of protein import translocons at the outer and inner

48   envelope membranes of chloroplasts – TOC and TIC, respectively (Jarvis and

49   López-Juez, 2013; Nakai, 2018; Richardson and Schnell, 2020).

50

51   At the outer membrane TOC complex, subunits with GTPase activity act as

52   receptors for the N-terminal targeting signals of chloroplast-destined

53   polypeptides, and another subunit, TOC75, acts as a transmembrane import

54   channel (Jarvis and López-Juez, 2013). At least two versions of the TOC

55   complex exist, with different client specificities: one contains receptors with a

56   preference for abundant photosynthetic pre-proteins, while the other favours

57   import of house-keeping pre-proteins, like those involved in the chloroplast

58   genetic machinery (Ivanova et al., 2004; Kubis et al., 2004; Jarvis and López-

59   Juez, 2013). Targeted replacement of TOC receptor proteins has been revealed

60   as a fundamental determinant of the development of photosynthetic or non-

61   photosynthetic plastids and of plastid type transitions (Ling et al., 2012; Ling et

62   al., 2019).

63

64   The identity of the inner membrane TIC components, in contrast, has been the

65   subject of considerable debate. Initial studies identified an abundant 110 kDa

66   protein (Kessler and Blobel, 1996; Lubeck et al., 1996), later named TIC110, and

67   postulated to be a scaffold coordinating internal chaperones (Inaba et al., 2003)

68   or, alternatively, the inner membrane import channel (Heins et al., 2002). Another

69   candidate for the role of inner membrane channel is TIC20 (Chen et al., 2002;

70 Kovacs-Bogdan et al., 2011), and a 1 MDa complex comprising nucleus-encoded

71 TIC20 and at least three other proteins – including TIC100, TIC56 and

72 chloroplast-encoded TIC214, but not including TIC110 – has been identified as a

73 core channel-forming TIC complex (Kikuchi et al., 2013). An alternative form of

74 TIC20 was shown to occur in root tissue, in the absence of the other components

75 of the complex. However, the 1 MDa TIC complex model has proven

76 controversial (de Vries et al., 2015; Nakai, 2015b; Bolter and Soll, 2017; Sjuts et

77 al., 2017; Richardson and Schnell, 2020). Objections center around the low

78 abundance of TIC20 compared to TIC110 (Vojta et al., 2004; Kovacs-Bogdan et

79 al., 2011), the fact that the three additional proteins of the 1 MDa complex are

80 absent in the grass family (Kikuchi et al., 2013; de Vries et al., 2015), the

81 observation that the full-length version of TIC56 is dispensable in Arabidopsis

82 (Kohler et al., 2015; Kohler et al., 2016; Schafer et al., 2019), and data pointing to

83 other functions for TIC56 and TIC214 (Kohler et al., 2016; Schafer et al., 2019).

84 The observation of a combined TOC-TIC "supercomplex" which includes TIC20

85 but also a small fraction of the total TIC110 (Chen and Li, 2017), leaves the issue

86 of the nature of the channel unresolved.

87

88 Chloroplast development in flowering plants occurs exclusively in the light

89 (Arsovski et al., 2012), because photoreceptors activate the expression of many

90 genes for chloroplast-destined proteins (Cackett et al., 2021). A genetic screen

91 for mutants in which light failed to activate the promoter of the *LHCB1*2* (*CAB3*)

92 gene led to the identification of *CAB-underexpressed* (*cue*) mutants (Li et al.,

93 1995; López-Juez et al., 1998). Among them, *cue8* exhibited a severe phenotype

94 characterised by reduced plastid development in both dark and light conditions,

95 and strongly impaired induction of (specifically) photosynthesis-associated genes

96 by phytochrome photoreceptors (López-Juez et al., 1998; Vinti et al., 2005) linked

97 to chloroplast-to-nucleus communication (Loudya et al., 2020). Seedlings of *cue8*

98 display largely normal photomorphogenesis but have leaf rosettes with a

99 virescent (slow-greening) phenotype. This virescence is due to a cellular

3

100 correction phenomenon: an "anterograde" (nucleus-to-chloroplast) response

101 which maintains a juvenile state of plastids, a delay in the transition from the pre-

102 photosynthetic proplastid to differentiated chloroplast state, manifested in multiple

103 physical and genetic features, and which allows for an eventual overcoming of

104 the plastid defect (Loudya et al., 2020). This change is a response to "retrograde

105 signals" (mediating chloroplast-to-nucleus communication), and can therefore be

106 described as a "retro-anterograde correction". Interestingly, evidence has

107 recently accumulated pointing to an involvement of defects affecting the import of

108 cytosol-synthesised proteins into chloroplasts (Wu et al., 2019; Tadini et al.,

109 2020), or protein folding or quality control inside the organelle (Tadini et al., 2016;

110 Wu et al., 2019; Tadini et al., 2020), in the initiation of changes in the cytosol.

111 Such processes are broadly described as protein homeostasis or "proteostasis",

112 and their involvement triggers what can be described as a folding stress

113 response, which may, in turn, cause retrograde signalling to the nucleus (Wu et

114 al., 2019; Tadini et al., 2020). Indeed, GUN1, a chloroplast pentatricopeptide

115 repeat protein which plays an important role in retrograde signalling, was shown

116 to interact with chaperones involved in, or acting after, protein import, with its

117 absence impairing import under specific conditions (Wu et al., 2019) and causing

118 some depletion of components of the import machinery itself (Tadini et al., 2020).

119

120 We sought the molecular identity of the *CUE8* gene by positional cloning. We

121 here report that *cue8* carries a missense mutation affecting TIC100, one of the

122 components of the 1 MDa TIC complex. Furthermore, a genetic screen for

123 suppressors of this mutant identified a second, intragenic mutation.

124 Comprehensive analyses of both *tic100^cue8* and the suppressed mutant (carrying

125 two mutations in the same gene) demonstrated a significant role for this protein in

126 chloroplast protein import, which is in turn consistent with such a role for the 1

127 MDa complex. In spite of the suppressed mutant's recovery in import capacity, it

128 retained a pronounced early virescence and exhibited strong genetic interaction

129 with the loss of GUN1. These results, alongside others showing changes in RNA

4

130   editing and gene expression and the likely occurrence of unimported

131   polypeptides, highlighted the dramatic impact that changes in TIC100 have on

132   chloroplast-to-nucleus communication.

133

134

135

136   **Results**

137

138   **Mutation of *CUE8* leads to defects in plastid development in leaves and**

139   **roots.**

140   The *cue8* mutant was previously identified following mutagenesis of the

141   pOCA108 reporter-containing line (Figure 1A) (Li et al., 1995). We recently

142   demonstrated that the virescent, slow-greening phenotype of *cue8* is associated

143   with reduced chloroplast development in early cotyledons or very young leaf

144   tissues (in which chloroplasts fail to fill the available cellular space), and by a

145   gradual recovery of normal chloroplasts (Loudya et al., 2020). We wished to

146   investigate whether the mutation impacts plastid development beyond leaves,

147   widely across tissues, and so incorporated a plastid-targeted DsRed fluorescent

148   protein (Haswell and Meyerowitz, 2006) into the wild type, and then introgressed

149   the transgene into the *cue8* mutant. The fluorescence signal was substantially

150   reduced in *cue8*, relative to wild type, both in cotyledon mesophyll cells and in

151   roots, in which partially-developed chloroplasts were prominent in cells

152   surrounding the central vasculature (Figure 1B and C). Accordingly, leaf

153   development and root elongation were both reduced in the mutant (Supplemental

154   Figure 1A and B). Supplementation of the growth medium with sucrose rescued

155   the *cue8* root phenotype, in a dose-dependent manner but to an incomplete

156   extent (Supplemental Figure 1). Thus, we concluded that CUE8 plays a role in

157   plastid development in non-photosynthetic tissues, as well as in photosynthetic

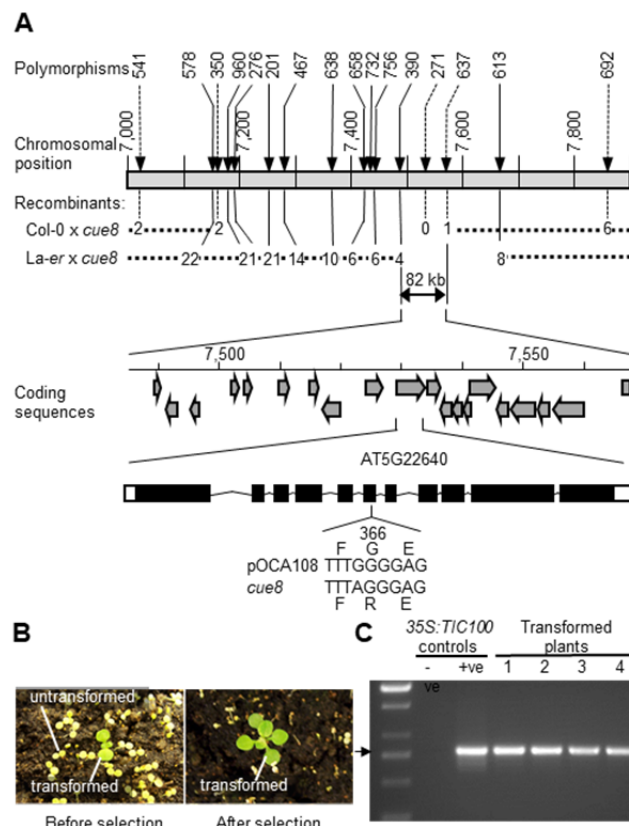158   tissues.

159

160

161

162
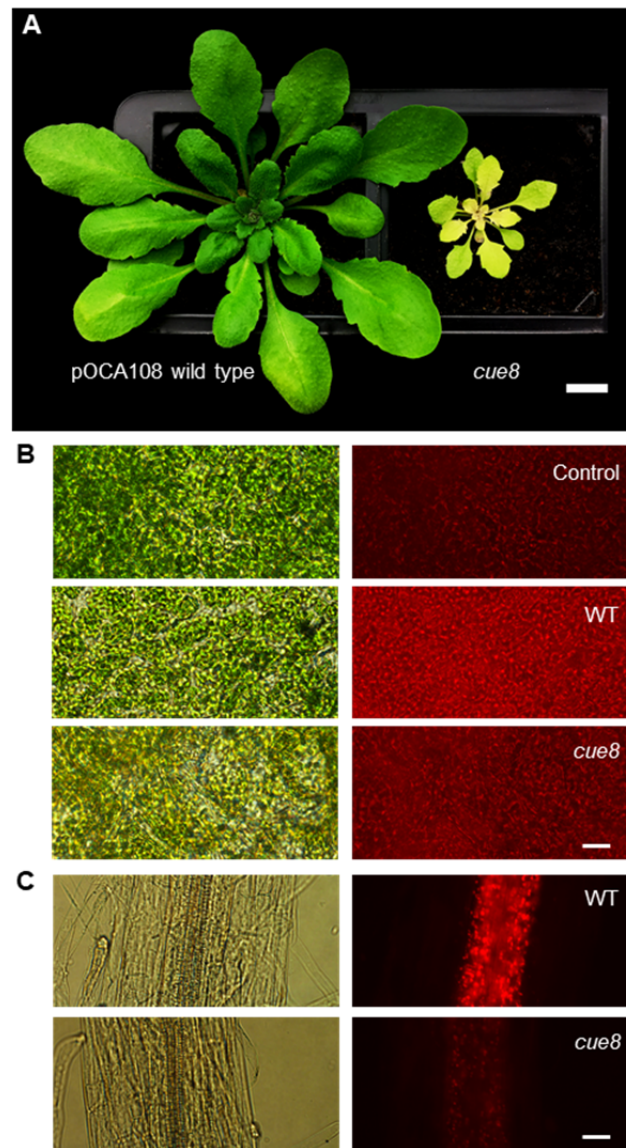
Figure 1. Mutation of *CUE8* causes a delay in plastid development in both aerial and root tissues. (**A**) Phenotype of 28-day-old pOCA108 wild type and *cue8* mutant plants. Scale bar 1 cm. (**B**) Mature cotyledon samples of plants without plastid-targeted dsRed (Control), or dsRed-containing pOCA108 wild type (5 days) or dsRed-containing *cue8* (6 days). (**C**) Root samples of equivalent seedlings. The same transgene was present in both genotypes, and images of WT and mutant were taken using the same exposure. Scale bar (**B** and **C**) 25 μm.

168 **Identification of the *CUE8* locus by linkage mapping.**

169 *cue8* and its wild-type progenitor (Li et al., 1995) are lines in the Bensheim

170 ecotype of Arabidopsis (Figure 1A). We generated two mapping populations for

171 *cue8* by performing outcrosses to both Landsberg-*erecta* (La-*er*) and Columbia

172 (Col-0), to take advantage of ecotype polymorphisms (Supplemental Table 1).

173 The *CUE8* locus was mapped to an 82 kb region of chromosome 5, containing 19

174 complete open reading frames (Figure 2A, see Materials and methods). A

175 Transformation-competent Artificial Chromosome (TAC) covering 11 of those

176 genes was able, when transformed into *cue8*, to complement the mutation

177 (Supplemental Figure 2 and Supplemental Table 2). A combination of

178 sequencing of individual candidate genes and assessment of the phenotypes of

179 T-DNA knockouts (Supplemental Table 2) ruled out 10 of those genes, while we

180 were unable to identify a viable homozygous mutant for AT5G22640 (only

181 heterozygous T-DNA-containing plants were recovered). Sequencing of genomic

182 DNA of *cue8* confirmed the presence of a mutation in this gene resulting in a

183 G→R amino acid substitution at position 366, just outside one of the protein's

184 predicted Membrane Occupation and Recognition Nexus (MORN) domains

185 (Takeshima et al., 2000) (Figure 2A, 5C, Supplemental Table 3). Transformation

186 of the mutant with a wild-type (pOCA108) cDNA encoded by AT5G22640 under

187 the control of a constitutive promoter also resulted in complementation (Figure 2B

188 and C). Thus, we concluded that *CUE8* is AT5G22640, a gene identified

189 previously as *EMB1211*, due to its embryo-lethal knockout mutant phenotype

190 (Liang et al., 2010), and, most interestingly, as *TIC100* (Kikuchi et al., 2013),

191 encoding a component of the putative 1 MDa TIC complex. We hereafter refer to

192 the mutant allele, and the plant carrying it, as *tic100^cue8*. Bearing in mind the

193 nature of the *tic100^cue8* amino acid substitution, as well as the mutant's virescent

194 phenotype, which contrasts with the loss of viability caused by a T-DNA insertion

195 at this locus, we concluded that the *tic100^cue8* is a hypomorphic allele, carrying a

196 missense mutation which causes a partial loss-of-function of the gene.

197

198   Several chloroplast protein import components have previously been shown to

199   have a preferential role in the import of either abundant, photosynthetic proteins

200   or less-abundant, but essential, plastid housekeeping proteins (Jarvis, 2008).

201   Having identified *CUE8*, we compared, using publicly-available data (Schmid et

202   al., 2005), its developmental expression with that of genes representative of

203   those two functions. The *CUE8*/*TIC100* gene exhibited (Supplemental Figure 3) a

204   combined expression pattern: high like *LHCB2.1* in photosynthetic tissues, while

205   also high like *TOC34* in those tissues rich in meristematic cells, such as the root

206   tip. Results of a search for co-regulated genes, using two different algorithms

207   (Supplemental Datasets 1 and 2) were also consistent with *CUE8*/*TIC100* being

208   involved early (for example, together with transcription and translation, pigment

209   synthesis and protein import functions) in the biogenesis of photosynthetic as

210   well as non-photosynthetic plastids.

211

212

Figure 2. Cloning of *CUE8*. (A) Map-based cloning of the *CUE8* gene, AT5G22640, encoding *TIC100* / *EMB1211*. Upper panel: abbreviated name of the polymorphisms used for mapping, position along chromosome 5 (in kb), and number of recombinants at those positions identified in the indicated mapping populations. This identifies an 82 kb region, containing 19 open reading frames (middle panel). A combination of strategies (Supplemental Table 2) identifies AT5G22640 (*TIC100*) as the *CUE8* locus, whose exon/intron structure is shown. A point mutation (lower panel) results in a single amino acid substitution (G366R) in the TIC100 protein sequence. **(B)** Complementation of *cue8* with *35S:TIC100*, carrying a *TIC100* cDNA under the control of a 35S promoter. Plants shown before and after the selection of transformants. **(C)** Diagnostic PCR confirming the presence of the *35S:TIC100* transgene in complemented plants. Positive (+ve) control, plasmid DNA harbouring the construct. Negative (-ve) control, DNA from plant prior to transformation.

222

223 **Reduced protein import rate and partial loss of the 1 MDa complex in**

224 *tic100^{cue8}* **chloroplasts.**

225 Taking advantage of the opportunity afforded by the partial loss of function of

226 TIC100 in *tic100^{cue8}*, we carried out *in vitro* import assays with chloroplasts

227 isolated from well-developed seedlings of the mutant, using a photosynthetic

228 protein precursor, the Rubisco small subunit (SSU). Four independent

229 experiments, using developmentally-comparable wild-type and mutant plants

230 (Figure 3A), revealed that *cue8* mutant chloroplasts import less than one-third of

231 the amount of pre-protein than the equivalent number of wild-type chloroplasts

232 (Figure 3B, C).

233

234 To understand more clearly the basis for the protein import deficiency in the

235 mutant, we analysed the levels of several translocon components by

236 immunoblotting. Equal amounts of total chloroplast proteins were loaded per

237 lane. Band intensities for some translocon components, in both the outer

238 (TOC75) and inner (TIC110, TIC40) envelope membranes, were elevated by

239 about a third in the *tic100^{cue8}* lanes (Supplemental Figure 4). This reflected the

240 fact that *tic100^{cue8}* chloroplasts are, to varying extents, less developed internally

241 and contain reduced amounts of the major photosynthetic proteins, including

242 Rubisco and LHCB (López-Juez et al., 1998), relative to wild type, leading to the

243 relative overloading of envelope components in the *tic100^{cue8}* samples when

244 using equal protein amounts (this also explains the slightly lower amounts of total

245 protein in the *tic100^{cue8}* samples following normalisation according to equal

246 chloroplast numbers in Figure 3B). Crucially, in spite of this, the level of TIC100

247 polypeptide was reduced to between one quarter and one eighth that in the wild

248 type (Supplemental Figure 4) on an equal total chloroplast protein basis, or less

249 than one eighth when normalized to another envelope protein, TIC40. The

250 decrease in TIC100 abundance in the mutant was linked to reductions in the

251 levels of the other components of the 1 MDa complex (TIC20 and the additional

252 TIC56 and TIC214; Supplemental Figure 4), to between 25 and 50% of wild-type

253   levels when expressed relative to TIC40. These observations are consistent with

254   the notion that these proteins associate, with the very substantial loss of

255   *tic100^{cue8}* preventing others from accumulating normally.
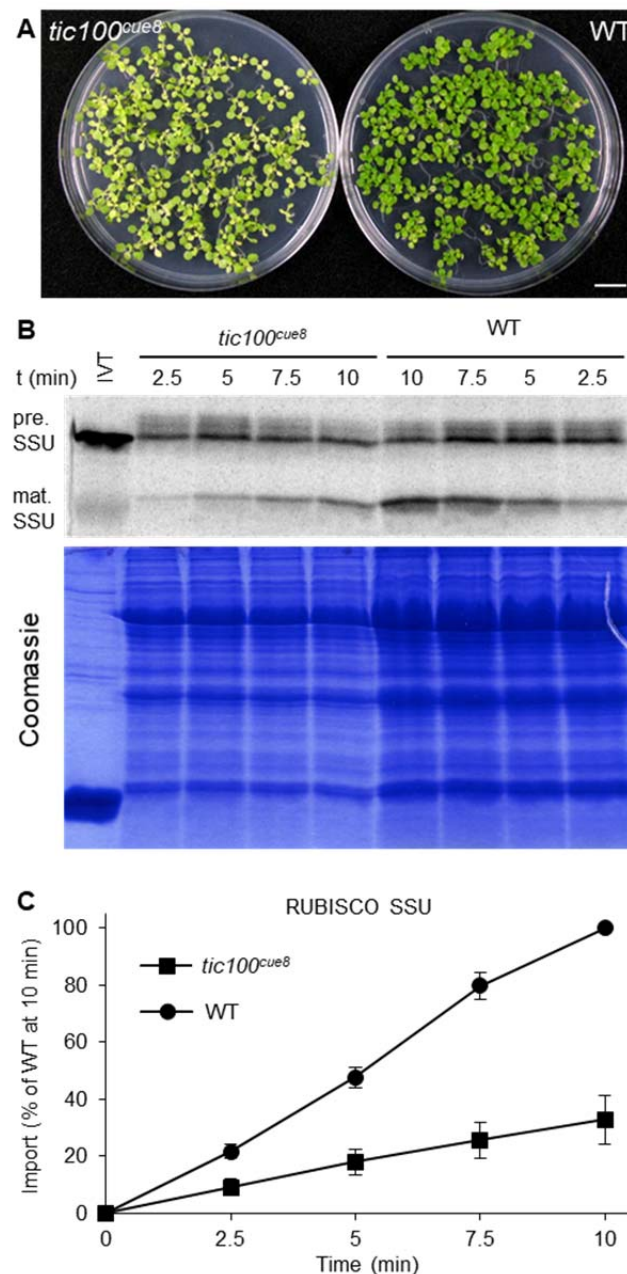
256

257

Figure 3. Chloroplasts of *tic100^cue8* exhibit reduced protein import rates. (A) 13-day-old wild-type and developmentally-comparable 17-day-old *tic100^cue8* mutant seedlings, used to isolate chloroplasts for import assays. Seedlings were grown on 0.5% sucrose. Scale bar: 1 cm. **(B)** Phosphor screen image of import reactions of *in vitro*-translated RUBISCO SSU polypeptide (IVT), carried out with equal total numbers of chloroplasts isolated from the seedlings above. Samples were taken 2.5, 5, 7.5 or 10 min after the start of the reaction. The import reaction converts the precursor (pre.) into mature polypeptide (mat.) of reduced size. Results from one representative experiment. A Coomassie-stained total protein gel corresponding to the same experiment is also shown. **(C)** Quantification of the amount of mature protein at each time point, normalised relative to the amount of mature protein in WT after 10 min of import. Average values from four independent experiments. Error bars represent s.e.m. Values for *tic100^cue8* were significantly different to those of WT at every time point (Student's t-test, 2-tailed, $p < 0.05$).

268

269

13

Identification of a suppressor mutation of *tic100^cue8*.

A search for suppressor mutations of the *ppi1* mutant, defective in the TOC33 subunit of the outer envelope translocon, led to the identification of SP1, a ubiquitin ligase which remodels the import complexes to control protein import and plastid development (Ling et al., 2012; Ling et al., 2019). We sought to deepen our understanding of inner envelope translocation processes by searching for suppressors of the *tic100^cue8* mutation. Screening of mutagenised M2 populations for increased levels of greening led to the identification of a mutant with a dramatic phenotype, which we named *suppressor of tic100 1*, *soh1* (Figure 4A). Backcrossing of *tic100^cue8 soh1* into the *tic100^cue8* parent resulted in 100% of the F1 (62 seedlings) showing a phenotype which was intermediate between that of the parents but closer to the *soh1* phenotype (Supplemental Figure 5A); while self-pollination of the F1 plants yielded 75% (554 out of 699, Chi-squared p=0.19) seedlings with suppressed phenotype, among which about a third displayed a marginally larger seedling phenotype (these plants represented a quarter of the total F2 population: 158 out of 699, Chi-squared *p*=0.21). These data indicated that *soh1* is a gain-of-function mutation that improves greening and growth, and which has a semi-dominant character.

We have recently shown that the virescent phenotype of *tic100^cue8* is caused by early chloroplasts in very young cotyledons being small and unable to fill the available cellular space (Loudya et al., 2020). In this regard, chloroplasts of 6-day-old *soh1* seedlings were much closer to those in the wild type (Figure 4B). Consequently, plastid DNA nucleoids, tightly packed in *tic100^cue8* as previously reported (Loudya et al., 2020), appeared much less dense in *soh1* (Figure 4C). Moreover, total chlorophyll of light-grown seedlings, protochlorophyllide of dark-grown seedlings, the average size of individual chloroplasts, and the mesophyll cellular occupancy by chloroplasts (the chloroplast index), which were all reduced dramatically in *tic100^cue8*, were largely restored in *soh1* seedlings (Figure 4D-G).
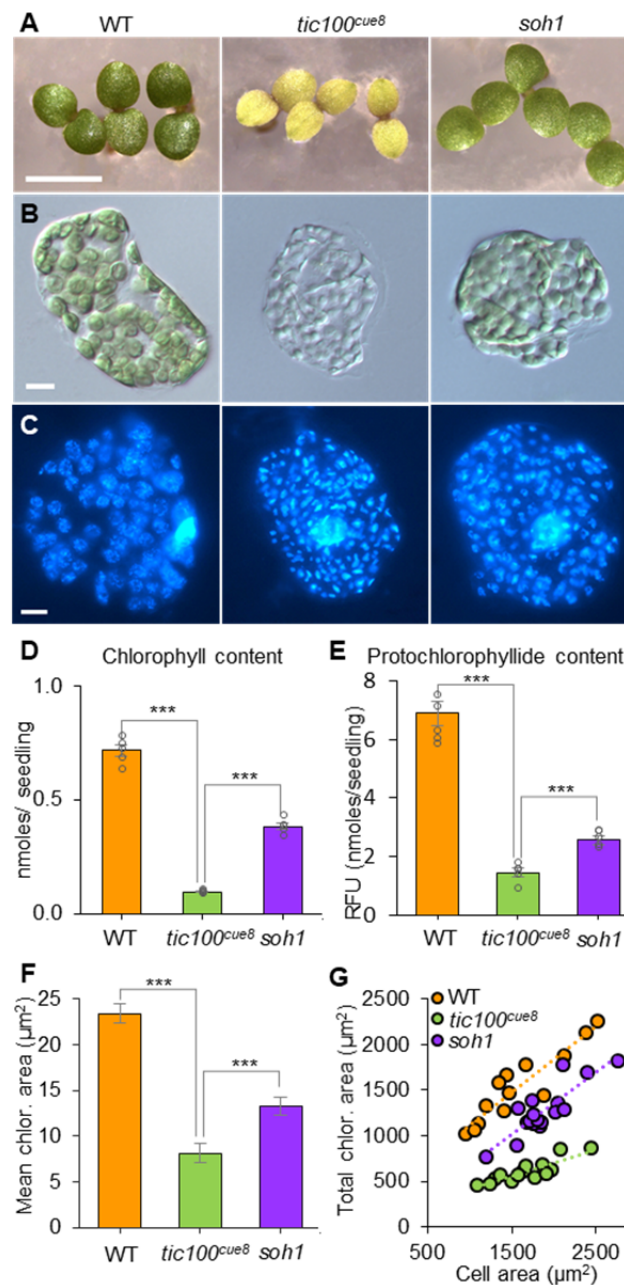
300

Figure 4. Identification of *soh1,* a suppressor mutant of *tic100^cue8^*, and phenotype of young cotyledon cells and their chloroplasts in wild type, *tic100^cue8^* and *soh1* seedlings. (A) Five-day (WT) and six-day (*tic100^cue8^* and *soh1*) seedlings. Scale bar: 5 mm. **(B)** Individual cells of the three genotypes, of seedlings equivalent to those in **A**, observed under DIC microscopy, displaying the different degrees of cell occupancy by chloroplasts. **(C)** Individual cells observed fluorescence microscopy following DAPI-staining of double-stranded DNA, revealing both the nuclei and the presence and density of nucleoids in individual chloroplasts. Scale bar (**B** and **C**) 10 μm. **(D)** Chlorophyll content per seedling for seedlings identical to those in **A**. **(E)** Protochlorophyllide content per seedling (RFU, relative fluorescence units) of 5-day-old seedlings of the three genotypes. **(F)** Mean area of individual chloroplasts in cells equivalent to those in **B**. **(G)** Total plan area of chloroplasts in a cell plotted against cell plan area, for the three genotypes, including regression lines of best fit. The presented values are means, and the error bars (in **D**, **E**) show s.e.m. from five biological replicates, each with at least 5 seedlings, or (in **F**) at least 10 individual chloroplasts from each of at least 13 individual cells total, obtained from at least four different cotyledons per genotype. For all panels, asterisks above lines denote comparisons under the lines: ***$P < 0.001$ (2-tailed Student's t-test).

15

Identification of the gene carrying the *soh1* mutation.

We generated a mapping population by backcrossing the suppressor mutant as originally identified (*tic100^cue8 soh1*, Bensheim ecotype) to the unmutagenised *tic100^cue8* parent (also in the Bensheim ecotype). F2 seedlings of unsuppressed, *tic100^cue8* phenotype were used for mapping by SHORT READS sequencing (SHOREmap) (Schneeberger et al., 2009), as described in Supplemental Figure 5B-C. Mapping of the *soh1* mutation identified a region of chromosome 5 (Supplemental Figure 5D) spanning seven genes with mutations in the open reading frame, and one of these was *TIC100*. Sanger sequencing confirmed the presence in the *soh1* mutant of both the original *tic100^cue8* mutation and a second mutation, which we provisionally named *tic100^soh1* (Figure 5A-C). Constitutive expression under the 35S promoter of a *tic100^cue8 soh1* cDNA carrying both of these mutations in the *tic100^cue8* mutant plants resulted in T1 plants showing a suppressed phenotype (Figure 5E); the genotyping of these plants confirmed the presence of both *tic100^cue8* (from the endogenous gene) and *tic100^cue8 soh1* alleles (from the transgene). In contrast, constitutive expression of the *tic100^cue8* cDNA under the same promoter in *tic100^cue8* plants produced only *tic100^cue8* phenotypes (Supplemental Figure 6), demonstrating that it was the second mutation, and not overexpression of the gene, that caused the suppression effect. Therefore, we concluded that the second mutation was indeed responsible for the suppressed phenotype, and we hereafter refer to the *tic100^cue8 soh1* double mutant as *tic100^soh1* (Figure 5A).

Analysis of the predicted domain structure of the TIC100 protein by searching in the Interpro domains database showed that the initial *tic100^cue8* mutation occurred immediately outside the C-terminus of the third of three MORN domains, introducing a basic arginine residue in place of a neutral glycine. Conversely, the *tic100^soh1* mutation replaced an arginine residue, within the third MORN domain (20 amino acids upstream of the *tic100^cue8* substitution), with a neutral glutamine residue (Figure 5B, C). Three-dimensional protein structure

16

344 prediction by the recent, breakthrough AlphaFold algorithm (Jumper et al., 2021)

345 indeed showed the aminoacids affected by the two substitutions to lie in very

346 close proximity in space, in regions of confidently predicted structure (Figure 5D),

347 at one end of a large, highly confidently predicted β-sheet region which includes

348 the MORN domains.

349

350 **TIC100^{cue8} and TIC100^{soh1} proteins retain localisation at the chloroplast**

351 **periphery.**

352 Previous biochemical analyses identified the TIC100 protein as part of the 1 MDa

353 complex in the inner envelope membrane with a proposed role in pre-protein

354 import (Kikuchi et al., 2013; Chen and Li, 2017; Richardson et al., 2018). In view

355 of the protein import defect of the mutant, described above, we asked whether

356 the *tic100^{cue8}* mutation interferes with the localisation of the TIC100 protein, and

357 whether such an effect might in turn be alleviated by the *tic100^{soh1}* mutation.

358 Therefore, we constructed YFP fusion versions of the TIC100 protein in its wild-

359 type and two mutant forms (the second carrying both mutations). Transient

360 overexpression of the fusions in protoplasts resulted in some accumulation of all

361 three proteins in the cytosol of the cells (Supplemental Figure 7), which interfered

362 with assessment of chloroplast envelope association. However, in protoplasts in

363 which rupture of the plasma membrane eliminated the background cytosolic

364 protein (which we interpret to be mislocalised owing to overexpression), TIC100

365 was clearly observed at the periphery of chloroplasts, possibly with a small

366 amount of intra-organellar signal; this is consistent with the previous

367 biochemically-determined localisation. Significantly, neither of the two mutations

368 altered this character (Figure 5F), and so we concluded that the mutations affect

369 a property of TIC100 other than its localisation.
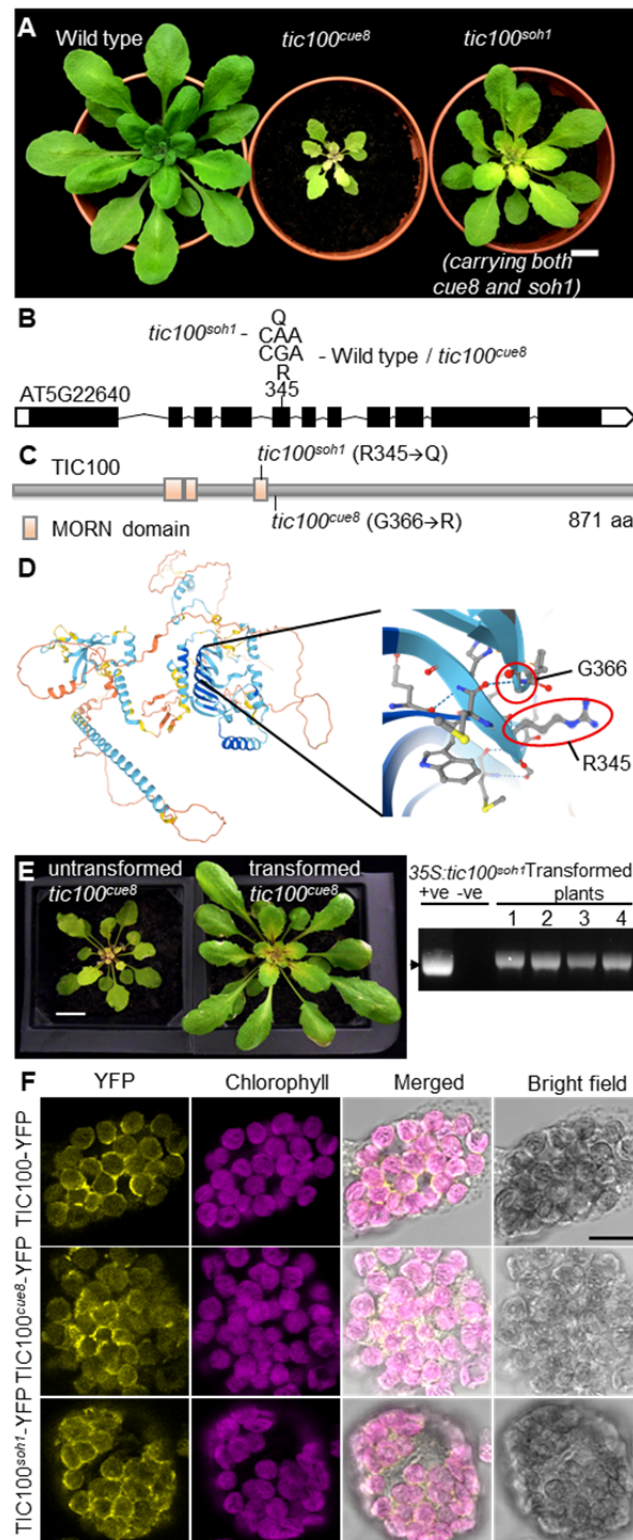
370

371

372

373

Figure 5. Cloning of the intragenic *suppressor of TIC100* (*soh1*) mutation, phenocopying and localization of TIC100. (A) Soil grown plants of wild type pOCA108, *tic100^{cue8}* (*tic100^{cue8}*) and suppressed *tic100^{cue8} soh1* double mutants (*tic100^{soh1}*) are shown at 28 days of age. Scale bar: 1 cm. **(B)** Second missense mutation (and resulting substituted aminoacid position) in the genomic sequence of the *TIC100* gene present in the *tic100^{soh1}* mutant and absent in *tic100^{cue8}* or its wild type parent. **(C)** Model of the domain structure of the TIC100 protein, indicating the position of the single mutation present in *tic100^{cue8}*, or the two mutations present in the *tic100^{soh1}* double mutant. The MORN domains occupy positions 219-239, 243-257 and 337-352. **(D)** TIC100 protein structure prediction by Alphafold, showing the position of the wild type aminoacids affected by the *tic100^{cue8}* and *tic100^{soh1}* mutations. Light and dark blue represent regions of confident and highly-confident prediction respectively. **(E)** Phenocopying of the suppressor *soh1* mutant by transformation of the single *tic100^{cue8}* mutant with an over-expressed, double-mutated *tic100^{soh1}* coding sequence driven by the 35S promoter (as seen in 11 independent T1 plants, 4 shown). Plants shown at 30 days of age. Scale bar: 1cm. Gel on the right confirms the genotype of the transformed plants. "+ve": positive genotyping control (bacterial plasmid). **(F)** Localisation of the TIC100 protein, in its wild type, TIC100^{cue8} and TIC100^{soh1} (double-mutated) forms, to the chloroplast periphery in transfected protoplasts. Wild-type protoplasts were transfected with constructs encoding wild-type and mutant forms of TIC100, each one tagged with a C-terminal YFP tag. The protoplasts were analysed by confocal microscopy. Images represent results of at least two independent experiments (at least 40 protoplasts per genotype) showing the same result. Scale bar: 10 μm.

19

393   ***tic100^soh1* corrects the protein import defect caused by *tic100^cue8*.**

394   Next, we asked whether the basis for the suppression of the *tic100^cue8* phenotype

395   in the *tic100^soh1* mutant was a correction of the plastid protein import defect

396   described earlier. In these experiments, the import of the photosynthetic SSU

397   pre-protein into equal numbers of chloroplasts isolated from wild-type, *tic100^cue8*

398   single-mutant, and *tic100^soh1* double-mutant plants (Figure 6A, B) was measured.

399   On this occasion, the results demonstrated a reduction of protein import in

400   *tic100^cue8* to approximately 55% of the wild-type level; the smaller reduction in

401   import seen here, relative to Figure 3, was attributed to the slightly greater extent

402   of development of the mutant plants on a higher sucrose concentration in the

403   medium (Supplemental Figure 1). Notably, protein import into the suppressed

404   mutant chloroplasts was restored almost completely to wild-type levels (over

405   90%) (Figure 6C, E).

406

407   To further assess the role of TIC100 in relation to functionally different proteins,

408   we additionally tested the import of the housekeeping plastid RPL11 protein (50S

409   plastid ribosomal subunit protein). This also allowed us to assess whether

410   reductions in import capacity in *tic100^cue8* chloroplasts could simply be an indirect

411   consequence of differences in the stage of development of mutant chloroplasts,

412   since SSU and RPL11 have been shown to be preferentially imported by

413   chloroplasts of younger or older leaves, respectively (Teng et al., 2012). To the

414   contrary, we obtained very similar results for RPL11 to those we had obtained for

415   SSU (Figure 6D, F).

416

417   Overall, these protein import data (which were observed across four independent

418   experiments per pre-protein) revealed a clear import defect in *tic100^cue8* for two

419   proteins which display different developmental stage-associated import profiles

420   (Teng et al., 2012), and which use different types of TOC complexes (Jarvis and

421   López-Juez, 2013; Demarsy et al., 2014). This was consistent with the gene

422   expression profile of *TIC100* (Supplemental Figure 3). Notably, this was also

423 consistent with the fact that SSU preprotein was previously shown to physically

424 associate during import with several components of the 1 MDa complex,

425 including TIC100, while RPL11 preprotein was found to associate with TIC214

426 (Kikuchi et al., 2018), Moreover, our results revealed a very pronounced

427 correction of the import defects seen in *tic100^cue8* chloroplasts in the *tic100^soh1*
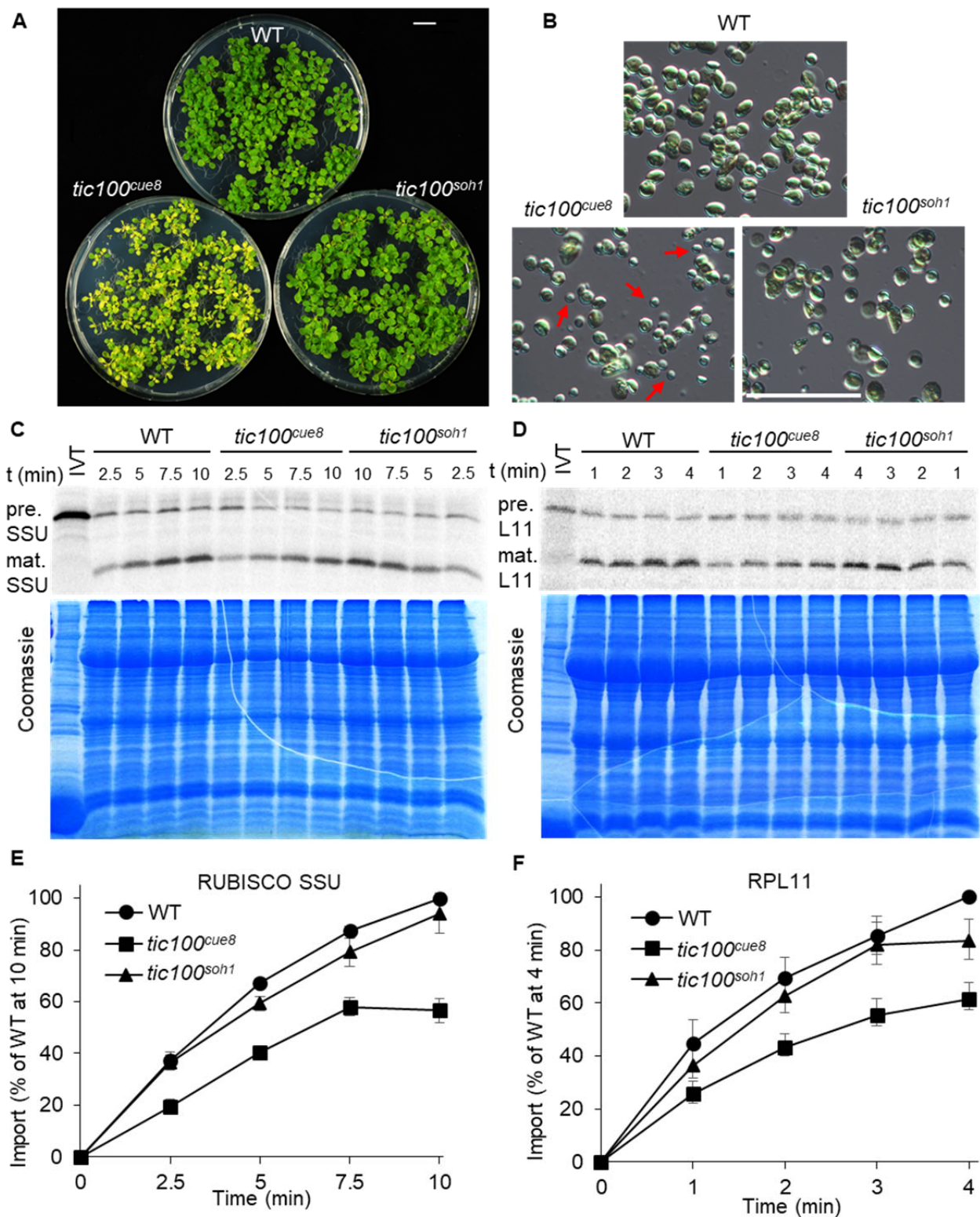
428 suppressed mutant.

429
430

431 **Figure 6. Chloroplasts of *tic100^cue8* exhibit reduced import of a photosynthetic and a housekeeping pre-protein,**
432 **with different age-dependent import profiles, and both defects are suppressed by the second mutation in**
433 ***tic100^soh1*. (A)** 13-day-old wild-type, and 17-day-old *tic100^cue8* and *tic100^soh1* mutant, seedlings used to isolate chloroplasts
434 for the import assays. Seedlings were grown on 1% sucrose. Scale bar: 1 cm. **(B)** Examples of chloroplast populations
435 used for the *in vitro* protein import assays. Occasional small chloroplasts in *tic100^cue8* are indicated with red arrows. Scale
436 bar: 50 μm. **(C)** Phosphor screen image of import reactions of *in vitro*-translated Rubisco small subunit (SSU) polypeptide
437 (IVT), carried out with equal numbers of *tic100^cue8* and wild-type chloroplasts. Samples were taken at the indicated times
438 after the start of the reaction. The import reaction converts the precursor (pre.) into the mature (mat.) polypeptide of
439 reduced size. Results from one representative experiment are shown. The lower panel shows the corresponding
440 Coomassie-stained total protein gel of the same experiment. **(D)** Import of RPL11 into equal numbers of wild type,
441 *tic100^cue8* and *tic100^soh1* chloroplasts. Upper and lower panels as in **C**. Values at every time point were significantly different
442 for *tic100^cue8* relative to WT, and for *tic100^soh1* relative to *tic100^cue8*. **(E)** Quantitation of at least four independent protein
443 import assays as that shown in **C**, from four separate chloroplast populations obtained from at least four groups of
444 independently grown plants. The presented values are means, and the error bars show s.e.m. **(F)** Quantitation of at least
445 four independent import assays, as that shown in **D**. Values at all time points for SSU and 2, 3 and 4 minutes for RPL11
446 were significantly different for *tic100^cue8* relative to WT, and for *tic100^soh1* relative to *tic100^cue8* ($p<0.05$, 2-tailed Student's t-
447 test).

448

449

450 ***tic100^soh1* restores levels of 1 MDa protein components in *tic100^cue8*.**

451 Given the strong reductions in levels of 1 MDa TIC complex components (but not

452 of other inner or outer envelope proteins) seen in *tic100^cue8* mutant chloroplasts

453 (Supplemental Figure 4), we asked whether the *tic100^soh1* mutation had corrected

454 the accumulation of components of the 1 MDa complex. Immunoblot analyses

455 indicated that this was indeed the case (Figure 7A-C). Analysis of TIC100 protein

456 using the same chloroplast preparations as used for import assays in Figure 6

457 showed partial restoration of the level of this protein in the double mutant.

458 Furthermore, qualitatively similar trends to those seen for TIC100 were observed

459 for TIC56 and TIC214, but we were unable to quantify TIC20 here due to very

460 limited availability of the corresponding antibody. In contrast, no such protein

461 level reduction in *tic100^cue8*, or restoration in *tic100^soh1*, was observed for control

462 housekeeping, non-membrane proteins (HSP70, RPL2); in fact envelope proteins

463 unrelated to the 1 MDa complex (TIC110, TIC40 and TOC75) appeared elevated

464 in *tic100^cue8*, consistent with an enrichment of envelope proteins per unit total

465 chloroplast protein, as discussed earlier, and accordingly returned to normal

466 apparent levels in *tic100^soh1*.

467

468 It could be argued that the reduced accumulation of the 1 MDa TIC might have

469 been an indirect result from a retrograde signalling impact of the *tic100^cue8*

470 mutation, leading to reduced nuclear gene expression and synthesis of

471 translocon components. Such an explanation is highly unlikely given that we

472 have previously observed elevated, not reduced, expression of nuclear and

473 chloroplast-encoded genes for early-expressed, plastid housekeeping proteins in

474 the mutant (Loudya et al., 2020). This is part of its "pre-photosynthetic, juvenile

475 plastid" phenotype. In fact, we confirmed here that the expression of nucleus-

476 encoded genes for 1 MDa TIC components and, especially, of the plastid-

477 encoded *tic214* gene, were all elevated in *tic100^cue8* (Figure 7D); the expression

478 of the control *TOC159* gene was also elevated. Interestingly, and as previously

479 observed for other elements of the juvenile plastid phenotype (Loudya et al.,

24

480   2020), a substantial component of the retro-anterograde correction did not

481   involve GUN1 action, since it occurred in *tic100^{cue8}* even in the absence of GUN1

482   (Supplemental Figure 8).

483

484   Moreover, the expression of *TIC20-IV*, which encodes an alternative form of

485   TIC20 that functions independently of the 1 MDa complex (Kikuchi 2013), was

486   also elevated in *tic100^{cue8}* (Figure 7D). Thus, we concluded that accumulation of

487   subunits of the TIC 1 MDa complex is reduced by the *tic100^{cue8}* mutation at the

488   posttranscriptional level, that this occurs in spite of the attempted "retro-

489   anterograde correction" at the gene expression level brought about by retrograde

490   signalling, and that the accumulation of TIC 1 MDa complex subunits is partially

491   restored by the *tic100^{soh1}* mutation. Furthermore, a potential compensatory effect

492   of the *tic100^{cue8}* mutation, increasing the expression of *TIC20-IV* encoding an

493   alternative TIC20 form that acts independently of the 1 MDa complex, is

494   apparent.

495
496
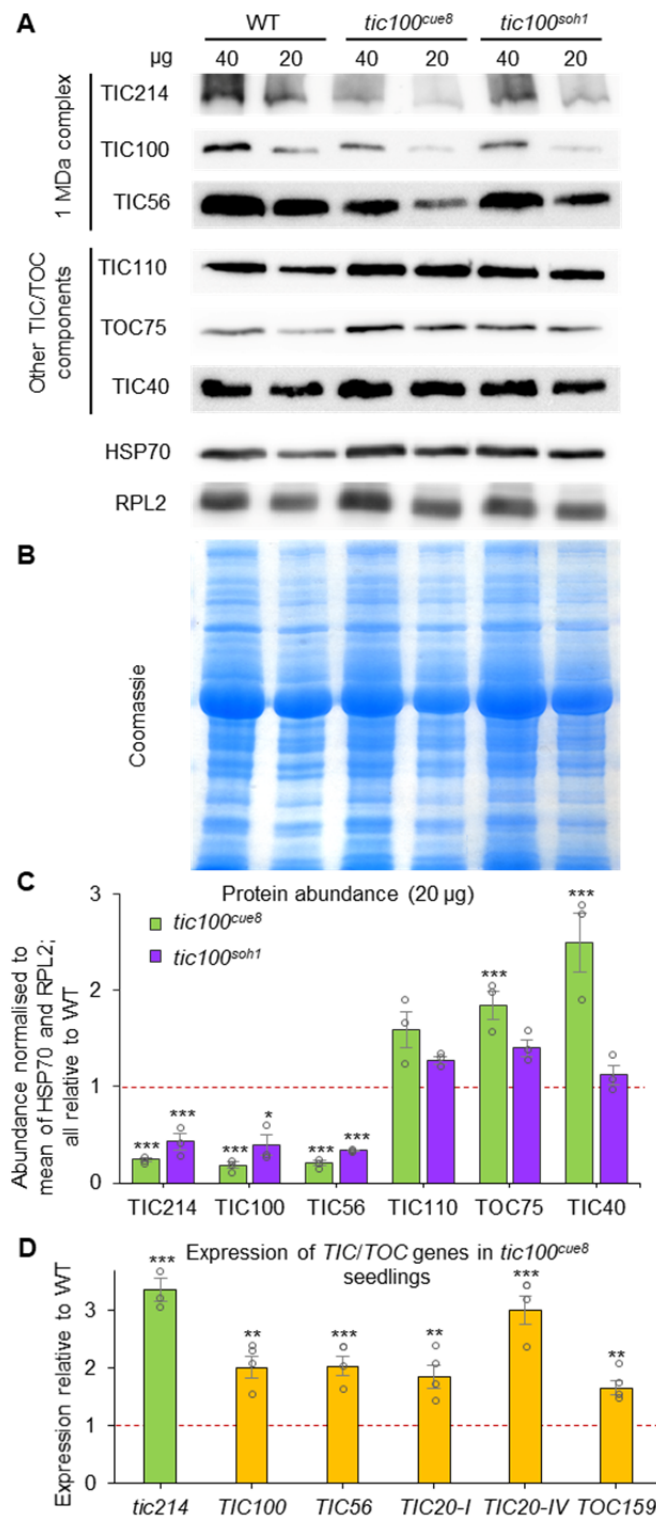
497 **Figure 7. Chloroplasts of *tic100^cue8^* display decreased levels of 1 MDa complex proteins specifically, and this**
498 **defect is suppressed by the second mutation in *tic100^soh1^*.** (A) Immunoblot analysis of total chloroplast proteins from
499 preparations from wild type (13-day-old), and *tic100^cue8^* and *tic100^soh1^* (17-day-old), seedlings (see Figure 6). The amount
500 of proteins (μg) loaded is indicated above each lane. The antibodies used for the detection of components of the 1 MDa
501 complex (TIC56, TIC100 and TIC214) or other chloroplast envelope proteins (TOC75, TIC40 and TIC110) are indicated.
502 Note the reduced amounts of components of the 1 MDa complex, which is apparent despite the increased loading of
503 envelope proteins (as revealed by the levels of other polypeptides) specifically in the *tic100^cue8^* samples. Very limited
504 antibody availability precluded probing the chloroplast protein extracts for the levels of TIC20. (B) Coomassie-stained total
505 protein gel of the same experiment. (C) Quantitation of protein abundance from an analysis of the 20 μg samples in three
506 independent experiments, relative to the mean of HSP70 and RPL2 in each sample, all expressed relative to wild-type
507 protein levels. The presented values are means, and the error bars show s.e.m. Asterisks represent significance of
508 difference of each mutant relative to WT (ANOVA followed by Dunnett's test). (D) Expression, measured by quantitative
509 real-time RT-PCR, of *TIC/TOC* genes in *tic100^cue8^* seedlings similar to those analysed in Figure 3, measured relative to
510 expression in wild-type seedlings. Note *tic214* is chloroplast-encoded. The presented values are means, and the error
511 bars show s.e.m. of three RNA samples (biological replicates), each with two technical replicates. Asterisks represent
512 significance of difference between mutant and WT: *P < 0.05, **P < 0.01, ***P < 0.001 (2-tailed Student's t-test). Dotted
513 lines represent protein levels (C) or expression (D) in WT.
514

515 ***Interplay between* tic100 *mutations and retrograde signalling.***

516 We previously observed that while the single *tic100^cue8^* mutation resulted in

517 virescence, the simultaneous loss of GUN1 (which in itself causes partial

518 uncoupling of nuclear gene expression from the state of the plastid) was

519 incompatible with survival – i.e., combination of the *tic100^cue8^* and *gun1* mutations

520 resulted in synthetic seedling lethality in the double mutants (Loudya et al.,

521 2020). To further investigate the extent of suppression in *tic100^soh1^*, we analysed

522 *tic100^soh1^ gun1* triple mutants. In contrast to *tic100^cue8^ gun1* albino, eventually

523 lethal mutants, the *tic100^soh1^ gun1* triple mutants were very pale but not lethal

524 (Figure 8A), and indeed they could survive and produce seeds entirely

525 photoautotrophycally under low light conditions. In other words, the synthetic

526 lethality of *tic100^cue8^ gun1* double mutants was suppressed by *tic100^soh1^*.

527

528 Evidence has recently accumulated for a role of altered organelle proteostasis in

529 chloroplast retrograde signaling (Tadini et al., 2016; Wu et al., 2019; Tadini et al.,

530 2020). The clear virescence exhibited by *tic100^soh1^*, and its strong, albeit reduced,

531 genetic interaction with loss of GUN1, led us to ask whether retrograde signalling

532 was in any way altered by impairment or recovery of TIC100 function. Two

533 scenarios were in principle possible: In the first, a strong response of reduced

534 photosynthesis-associated nuclear gene (PhANG) expression might be observed

535 when TIC100 function is reduced, resulting in the virescence of *tic100^cue8^* and

536 even *tic100^soh1^* mutants, and the very low PhANG expression in *tic100^cue8^* (Vinti

537 et al., 2005),. In this scenario, GUN1 function, mediating retrograde signalling,

538 would remain fundamentally unchanged in the mutants. In the second scenario,

539 the impairment of protein import occurring in *tic100^cue8^*, but barely so in *tic100^soh1^*,

540 would result in the accumulation of unimported proteins in the cytosol of the

541 mutants, and this in turn, as proposed by Wu and coworkers (Wu et al., 2019),

542 would itself cause elevated PhANG expression in spite of the chloroplast

543 damage, i.e., a *genomes uncoupled* (*gun*) phenotype. We examined these two

544 possible, contrasting scenarios by quantifying transcript levels of *LHCB1.2*,

28

545   *RBCS* and *CA1* – the first two genes classically monitored in retrograde

546   analyses, and the third gene showing one of the greatest extents of reduction by

547   treatment with lincomycin (Koussevitzky et al., 2007) – in the presence of a

548   chloroplast translation inhibitor which triggers a dramatic loss of PhANG

549   expression. We exposed to lincomycin seedlings of each *tic100* mutant, and of

550   the *tic100^soh1^ gun1* triple mutant. We did not examine *tic100^cue8^ gun1*, as such

551   albino seedlings become impossible to select in the presence of the antibiotic

552   from the segregating population in which they occur. The results of this analysis

553   (Figure 8B-C) are clearly consistent with the first scenario: reductions in PhANG

554   expression were strong in the absence of lincomycin in *tic100^cue8^ gun1* double

555   and in the *tic100^soh1^ gun1* triple mutants (Figure 8B), and mild in *tic100^soh1^*. The

556   reductions in the double mutant were not due to the *gun1* mutation having lost its

557   associated "uncoupled" phenotype, but rather to the very strong chloroplast

558   defect (manifested as a greening defect) in the double. This was shown by the

559   fact that in *tic100^soh1^ gun1* PhANG expression, particularly that of *CA1*, was

560   clearly uncoupled, i.e., much less reduced by lincomycin than it was in the wild

561   type (Figure 8C). We concluded that, as anticipated, *tic100^cue8^* is not a *gun*

562   mutant. We also concluded that the capacity of GUN1 to initiate retrograde

563   communication remains strong in *tic100^soh1^*, and that it can therefore explain the

564   retained, pronounced virescence.

565

566   PhANG expression changes, in particular in seedlings grown on lincomycin, have

567   been attributed to the presence of unimported precursor proteins, which can be

568   detected in whole-cell and cytosolic extracts of such antibiotic-treated plants (Wu

569   et al., 2019; Tadini et al., 2020). Such precursors have also been detected in

570   *gun1* even in the absence of antibiotic (Tadini et al., 2020), and it was reasonable

571   to speculate that they might be also detectable in the *tic100* mutants. We

572   examined this through immunoblot analysis of the FtsH2 protein, a thylakoid-

573   associated chaperone for which high molecular weight (HMW) bands have been

574   previously observed (Tadini et al., 2020) using the same antibody. The HMW

575   bands were previously shown to represent cytosolic, unimported precursors by

576   cellular fractionation and by the construction and examination of FtsH2-GFP

577   fusion proteins. Our results (Figure 8D) confirmed that the level of mature FtsH2

578   protein is much reduced in extracts of lincomycin-treated seedlings. Furthermore,

579   the antibody could detect the presence of the same HMW bands (unimported

580   protein) in extracts of seedlings grown in the presence of the antibiotic, and also

581   in those of mutant seedlings in its absence, an observation which is consistent

582   with a chloroplast protein import defect in both cases.

583

584

586
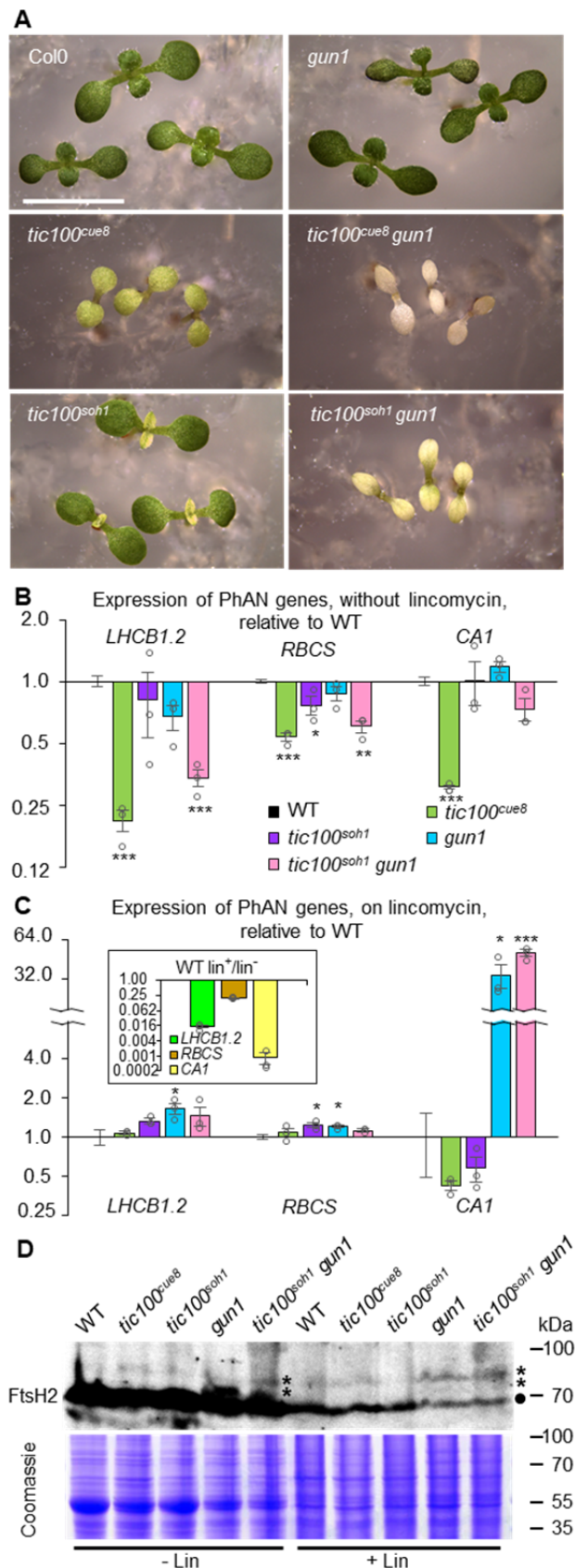
Figure 8. The *tic100^soh1* mutation suppresses the synthetic seedling lethality of *tic100^cue8* in combination with *gun1*, while *gun1* retains its "uncoupled" phenotype and unimported FtsH2 precursors can be detected in the *tic* mutants. (A) Phenotype of 7-day-old seedlings of the genotypes indicated. *tic100^cue8 gun1* double mutants exhibit eventual seedling lethality. Scale bar: 5 mm. **(B, C)** Photosynthesis-associated nuclear (PhAN) gene expression in the absence **(B)** or presence **(C)** of lincomycin in the genotypes indicated. Asterisks denote significance of difference between mutant and WT as indicated for Figure 7D. The inset compares the phenotype of the wild type grown on lincomycin with that in its absence. Differences for all three genes exhibited P < 0.001. **(D)** Immunoblot detection of higher molecular weight bands, previously shown to represent unimported, cytosolic precursors (asterisks) of chloroplastic FtsH2 (circle), in the presence or absence of lincomycin, in the genotypes indicated.

596

597

598   Editing of chloroplast mRNA is altered in *tic100^{soh1} gun1* seedlings in a

599   manner consistent with the juvenile plastid phenotype.

600   RNA editing occurs for many chloroplast transcripts, and it has been previously

601   demonstrated that growth of seedlings on norflurazon (which blocks carotenoid

602   synthesis) or lincomycin, and the concomitant disruption of chloroplast

603   development, results in changes in the extent of editing of different chloroplast

604   transcripts (Kakizaki et al., 2012). Importantly, such changes, involving both

605   increases and decreases in editing, were also observed in plants defective in the

606   TOC159 outer membrane translocon receptor (Kakizaki et al., 2012). They were

607   also seen in *tic100^{cue8}* and, even more dramatically, *tic100^{cue8} gun1* (Loudya et

608   al., 2020); and they involved increased editing of *rpoC1*, encoding a subunit of

609   the chloroplast RNA polymerase, and decreased of *ndhB*, encoding a

610   photosynthetic electron transport protein. We interpreted such changes, not as

611   evidence of a direct role of CUE8 (TIC100) in editing, but as part of the "juvenile

612   plastid" phenotype of the mutants. That interpretation is consistent with the

613   existence of two phases of organelle biogenesis: an early, "plastid development"

614   phase (photosynthesis-enabling but pre-photosynthetic, involving expression of

615   the chloroplast genetic machinery), and a later, "chloroplast development" phase

616   involving photosynthetic gene expression (as seen particularly clearly in

617   developing cereal leaves: (Chotewutmontri and Barkan, 2016; Loudya et al.,

618   2021). We asked whether this aspect of the *tic100^{cue8}* phenotype had also been

619   suppressed by *tic100^{soh1}*. This was indeed the case (Figure 9): the extent of

620   editing of *rpoC1* and *ndhB* transcripts was indistinguishable between *tic100^{soh1}*

621   and the wild type (or *gun1*). In contrast, editing was increased for *rpoC1*, and

622   reduced for *ndhB*, in the *tic100^{soh1} gun1* double mutant, which we again interpret

623   as a more juvenile state of chloroplast development caused by the combination

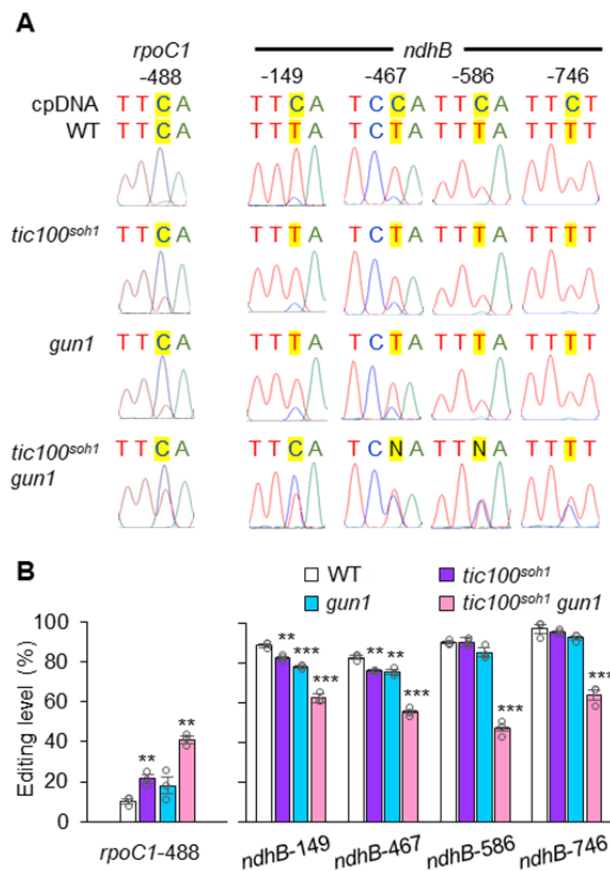624   of the mild loss of import capacity and the simultaneous loss of GUN1 function.

Figure 9. Editing of chloroplast mRNA is increased for the transcripts of *rpoC1* and decreased for those of *ndhB* in *tic100^soh1^ gun1* seedlings. (A) Representative sequence electropherograms of cDNA generated from cDNA of the genotypes indicated. The original, genomic cpDNA sequence is indicated at the top. **(B)** Quantitation of the degree of editing of the two plastid mRNAs shown in **(A)**, averaged for three independent cDNA preparations from different seedling samples per genotype. Asterisks denote significance of difference between mutant and WT as indicated for Figure 7D.

34

635 **Discussion**

636 The nature of the proteins imported into plastids clearly determines plastid type

637 and functions, and the identity of the import receptors even influences whole-

638 plant performance in the face of stress. This underscores the importance of

639 questions concerning the exact composition of the protein translocons. Indeed,

640 the identity of the inner membrane TIC machinery has been the subject of much

641 debate, particularly concerning the identity of the channel and the import motor

642 (de Vries et al., 2015; Nakai, 2015b; Bolter and Soll, 2017; Sjuts et al., 2017;

643 Schafer et al., 2019; Nakai, 2020; Richardson and Schnell, 2020). The

644 serendipitous identification of *cue8* as a hypomorphic allele of *TIC100* provided

645 an opportunity to begin addressing one such area of controversy. Knockout

646 mutants of *TIC100*/*EMB1211* (a component of TIC 1 MDa complex) suffer from

647 severe embryo development defects, leading to very early seedling lethality

648 (Liang et al., 2010; Kikuchi et al., 2013). Attempts have previously been made to

649 address the role of the 1 MDa complex by assessing the import characteristics of

650 the seedling-lethal knockout mutant *tic56*-1, by proteomically analysing

651 chloroplast-targeted proteins in such seedlings (Kohler et al., 2015). However

652 such analysis is indirect and cannot, by definition, reveal differences in import

653 rate, since seedlings are examined after lengthy *in vitro* culture. A second mutant,

654 *tic56*-3, expresses a truncated TIC56 protein and has a mild phenotype, allowing

655 the execution of *in vitro* assays to determine chloroplast protein import rates

656 (Kikuchi et al., 2013; Kohler et al., 2015). Perhaps owing to different growth or

657 chloroplast preparation conditions, those experiments did (Kikuchi et al., 2013) or

658 did not (Kohler et al., 2015) observe reduced import rates in the mutant. In fact,

659 one analysis reported very low levels of 1 MDa complex subunits overall in the

660 *tic56*-3 mutant, and failed to detect TIC100 at all (Schafer et al., 2019), while in

661 the same mutant TIC100 had previously been readily observable (Kikuchi et al.,

662 2013). Understandably, it has been difficult to reach consensus based on data

663 obtained from such genotypes.

664

665   An alternative approach may help to provide a resolution. Informative *in vitro*

666   protein import rate assays were readily performed in the current study using the

667   chloroplasts of *tic100^{cue8}*, which are severely impaired in TIC100 accumulation

668   due to the *tic100^{cue8}* mutation. Our data demonstrated a clear reduction in the

669   efficiency of protein import into mutant chloroplasts, which cannot be explained

670   simply by their reduced size or extent of development. Importantly, we have

671   previously observed a physical and gene expression phenotype consistent with a

672   juvenile state of plastid development in *tic100^{cue8}* plastids (Loudya et al., 2020),

673   and it is well known that plastids of young plants generally achieve greater, not

674   inferior, import efficiencies (Dahlin and Cline, 1991). The use of two different

675   preproteins with different age-dependency of import profiles (Teng et al., 2012;

676   Chu et al., 2020), both of which exhibited reduced import in *tic100^{cue8}*, indicated

677   that the import reduction was not an indirect consequence of an altered

678   developmental stage of the mutant organelles. On the contrary, the reduced

679   protein import seen in *tic100^{cue8}* chloroplasts provided a clear molecular

680   explanation for the mutant's strongly virescent phenotype; while the increased

681   rate of protein import seen in *tic100^{soh1}* chloroplasts explained the reduction of

682   this virescence. We should stress that the suppressor mutation present in

683   *tic100^{soh1}* is unlikely to, in itself, have a positive impact on TIC100 function. It

684   rather removes a native positive charge present in very close proximity to the

685   additional positive charge introduced by the *tic100^{cue8}* mutation. The suppressor

686   mutation is therefore likely to have removed an electrostatic repulsion present in

687   the *tic100^{cue8}* mutant protein, which allowed the conformation of TIC100 to return

688   to a mildly-impaired state, close to its native one.

689

690   The link between the abundance of TIC100 and that of its putative 1 MDa

691   complex partners, in both *tic100^{cue8}* and the intragenic suppressor mutant

692   *tic100^{soh1}*, is consistent with the existence of this complex. Furthermore, the

693   protein accumulation profile data revealed a correlation between protein import

694   rates and 1 MDa complex protein levels: decreased (*tic100^{cue8}*) or increased

695   (*tic100^soh1*) protein import rates were observed as subunits of the complex

696   decreased (*tic100^cue8*) or increased (*tic100^soh1*), in a genetically-determined

697   manner. The data further showed that some loss of the subunits, as seen in

698   *tic100^soh1*, can be tolerated with minimal deleterious impact on protein import at

699   the chloroplast-containing seedling stage; an equivalent phenomenon could

700   potentially explain some of the previous conflicting observations on *tic56*-3. Thus,

701   our data are consistent with the existence of the TIC100-containing 1 MDa

702   complex and with it having a role in protein import. Our results also confirm the

703   need for the complex for the normal import of different types of pre-proteins,

704   exemplified by Rubisco SSU, a model photosynthetic protein, and RPL11, a non-

705   photosynthetic protein. Nonetheless, we emphasise that the data presented here

706   do not in any way rule out an important role for TIC110 in protein import; for

707   example, this protein may function at a later stage in the import process, by

708   providing a scaffold for the coordination of stromal chaperones as previously

709   proposed (Inaba et al., 2003; Jarvis and López-Juez, 2013; Tsai et al., 2013;

710   Richardson and Schnell, 2020).

711

712   Among the difficulties raised concerning the proposed role of the 1 MDa complex

713   in protein import, one is of a phylogenetic nature: the absence of several of the

714   complex's main components from the grass family of monocots (de Vries et al.,

715   2015; Bolter and Soll, 2016). In contrast, recent evidence strongly supports the

716   function of the complex in a chlorophyte alga (Ramundo et al., 2020). It has been

717   argued that an alternative form of the TIC20 translocon may operate in grasses,

718   and that this utilises orthologues of TIC20-IV which is expressed and presumably

719   active in roots of Arabidopsis (Kasmati et al., 2011; Nakai, 2015a). In this light, it

720   is worth noting that the developmental impairment seen in roots of *tic100^cue8* was

721   not as pronounced as that observed in shoot meristem-derived tissues,

722   suggesting a reduced need for TIC100 in the roots compared to shoots.

723   Interestingly, we observed in *tic100^cue8* a three-fold increase in expression of

724   *TIC20-IV*. This may be a compensation for the loss of function of TIC20-I that

37

725 occurs in the absence of its 1 MDa partners, as the level of expression of *TIC20-I*

726 is four-fold higher than that of *TIC20-IV* in emerging seedling cotyledons and six-

727 fold higher in young leaves (Klepikova et al., 2016). TIC20-IV, independent of the

728 1 MDa complex, might have also escaped the obvious posttranscriptional

729 regulation we observed for components of the complex in the *tic100^cue8* mutant.

730 Nevertheless we do not believe that TIC20-IV could fully compensate for defects

731 in 1 MDa complex, given the lethality of complex knockout mutants. It is apparent

732 that there are some unquestionable differences between grasses and the

733 majority of other flowering plant groups in terms of chloroplast biogenesis in

734 leaves. For example, while the greening of dicot leaf primordia is noticeable from

735 the very youngest stages, the greening of grass leaves occurs over a longer

736 developmental period. Differences have also been seen for otherwise important

737 components involved in organelle biogenesis; for example grass family genomes

738 contain genes for one chloroplast-targeted and one mitochondrion-targeted RNA

739 polymerase, but no gene for a protein targeted to both, whereas dicots do carry

740 such a dual-targeted enzyme (Borner et al., 2015).

741

742 At present we can only speculate on the specific role of TIC100 within the 1 MDa

743 complex. The nature of the *soh1* mutation highlighted the importance of at least

744 one of the three recognised MORN domains in the protein. Such domains have

745 been shown to be important in other proteins for membrane association and for

746 association with specific lipids (Takeshima et al., 2000). Previous experiments

747 (Kikuchi et al., 2013) have revealed that this protein, like TIC56, most likely

748 occupies an intermembrane space position associated with the inner envelope

749 membrane, while TIC20 (the protein with channel properties (Kovacs-Bogdan et

750 al., 2011)) and TIC214 are integral membrane proteins. Our study also confirmed

751 a localisation consistent with envelope association for TIC100, and one may

752 speculate that this association is partly mediated by the MORN domains.

753 However, our confocal microscopy analysis did not reveal any change in

754 localisation in the TIC100^cue8 and TIC100^soh1 mutant proteins. Therefore, we

38

755   interpret that the mutations either affect or rescue some other aspect of TIC100

756   function, such as interactions with other members of the 1 MDa complex to

757   promote complex stability.

758

759   A role (possibly an additional one) for TIC56 in chloroplast ribosome assembly

760   has been reported, and mild translation inhibition phenocopies many aspects of

761   the *tic56*-3 phenotype (Kohler et al., 2016). These observations have been raised

762   as an objection against the involvement of the TOC56 protein, and by extension

763   of the 1 MDa complex, in protein import. However, intriguingly, such translation

764   inhibition also phenocopies the phenotype caused by the loss the receptor

765   protein TOC159, which has an extremely well established role in import (Kohler

766   et al., 2016). Reduced accumulation of two import-related but chloroplast-

767   encoded proteins, TIC214 and Ycf2/FtsHi – the latter a subunit of a putative

768   import motor (Kikuchi et al., 2018) – might explain such similarities.

769

770   Intriguingly, *tic100^{soh1}* exhibited almost complete rescue of protein import rates

771   and of greening in fully-developed leaf tissue, and yet it still displayed a

772   pronounced, early virescence phenotype. This virescence is consistent with a

773   strong early impact on plastid-to-nucleus communication (a strong early

774   retrograde signal, should the signal be a negative regulator of photosynthetic

775   gene expression; or a strong absence of one, should the signal be a positive

776   regulator). Indeed, the *tic100^{soh1} gun1* double mutant was very severely

777   greening-deficient, although not seedling lethal. Combined loss of TOC159 and

778   GUN1 has also been reported to have severe consequences (in this case,

779   seedling lethality) (Kakizaki et al., 2012). A number of important connections

780   between GUN1 and the chloroplast protein import apparatus have recently been

781   uncovered. *gun1* mutants lose subunits of the import translocons, including

782   TIC100, in response to mild inhibition of chloroplast translation, to a greater

783   extent than the wild type does (Tadini et al., 2020). A 50% reduction in levels of

784   import translocon subunits in *gun1*, observed on antibiotic-free medium (Tadini et

785 al., 2020), could have made seedlings somewhat more sensitive to the defects

786 brought about by the *tic100* mutations. However, that cannot fully explain the

787 very strong genetic interactions between the respective mutations, reaching

788 seedling lethality in the case of *tic100^{cue8} gun1*. *gun1* also causes mild but

789 synergistic decreases in import rates in a mutant defective in chloroplast

790 proteostasis, and GUN1 physically associates with chloroplast chaperones that

791 act in protein import (Wu et al., 2019). Both of those studies (Wu et al., 2019;

792 Tadini et al., 2020) demonstrated the accumulation of unimported preproteins in

793 the wild type in the presence of lincomycin, and in *gun1* even in its absence. We

794 observed HMW bands of FtsH2 that likely represent such unimported

795 preproteins, and could particularly detect such bands in young seedlings of the

796 mutant *tic100* genotypes, further supporting the import defects occurring in them.

797 (Wu et al., 2019) also observed the emergence of a cellular folding stress

798 response in the cytosol of chloroplast proteostasis mutants, consistent with the

799 presence of such unimported proteins. We should note, though, that our

800 evidence is consistent with the accumulation of unimported preproteins in the

801 cytosol playing a major signalling role which results in the reduction, not the

802 maintenance, of PhANG expression. The reduction in PhANG expression in

803 response to impairment of TIC100 function particularly in *tic100^{cue8}*, or to

804 exposure to lincomycin, both of which may or do lead to preprotein accumulation,

805 is consistent only with such a negative role. Therefore, our data do not support

806 this aspect of the previously proposed model (Wu et al., 2019), of a role for

807 increased accumulation of preproteins in elevating PhANG expression and

808 therefore being the cause of the *gun* phenotype in the *gun1* mutant. We also did

809 not observe a *gun* phenotype in *tic100^{cue8}*, nor, in fact, was a *gun* phenotype

810 observed in *toc33* (*ppi1*), *toc75-III*-3 and *tic40*-4 mutants (Wu et al., 2019). Our

811 data support a loss of protein import at the inner envelope bringing about a

812 reduction in PhANG expression and triggering a retro-anterograde delay in

813 chloroplast development which requires GUN1 and, by allowing gradual

814 correction of the defect, has adaptive value (Loudya et al., 2020). Our previous

815   and current data on RNA editing in *tic100* mutants also support the notion that

816   the shifts in degree of RNA editing occurring for different chloroplast transcripts

817   also constitute part of such a retro-anterograde correction.

818

819   Taking these observations together, it is becoming apparent that the status of

820   organelle protein import – particularly at the inner envelope membrane, mediated

821   by the 1 MDa TIC complex – and protein homeostasis are critically interlinked

822   with intracellular communication, and monitoring them is a critical function of

823   chloroplast retrograde signalling, and of the GUN1 protein specifically. According

824   to our observations, and consistently with previous ones (Kubis et al., 2003),

825   impaired protein import reduces PhANG expression. How GUN1 relays

826   information of changes in import status appears to remain unresolved, and

827   warrants future exploration.

828

829

830

831 **Methods**

832

833 **Plant material and growth conditions**

834 The *Arabidopsis thaliana cue8* mutant (López-Juez et al., 1998; Vinti et al., 2005)

835 and its wild type pOCA108, in the Bensheim ecotype, have been described. The

836 *gun1*-1 mutant, in the Col-0 ecotype, was previously described (Susek et al.,

837 1993).The *cue8* and *soh1* mutations were backcrossed into Col-0 for double

838 mutant analysis as described (Loudya et al., 2020). The generation of the *soh1*

839 mutant is described below. Plants were grown in soil under 16 h photoperiods

840 and a fluence rate of 180 µmol m^{-2} s^{-1}, and seedlings grown *in vitro* in MS media

841 supplemented with 1% sucrose, unless otherwise indicated (Supplemental Figure

842 1) under continuous white light, at a fluence rate of 100 µmol m^{-2} s^{-1}, as

843 previously described (López-Juez et al., 1998; Loudya et al., 2020). Genotyping

844 of the individual mutations (following gene identification), individually or for

845 double mutant generation, used PCR followed by restriction digestion

846 (Supplemental Table 4).

847

848 **Analysis of plastid development**

849 Wild type and *cue8* lines carrying the DsRed reporter gene targeted to

850 chloroplasts (Haswell and Meyerowitz, 2006) were identified following a cross

851 and selected to homozygosity. Cotyledons and roots from *in vitro*-grown

852 seedlings (7-day-old) were mounted on slides and observed using a Nikon

853 (Kingston upon Thames, UK) Eclipse NI fluorescence microscope, x20 Plan Fluor

854 objective and Texas Red filter block. Cotyledons of non-DsRed, negative control

855 seedlings were examined to confirm that the majority of the fluorescence signal

856 was attributable to the DsRed plastid reporter (Figure 1). Fluorescence images of

857 the same type of tissue used identical exposure conditions.

858 Five-day-old wild type and six-day-old mutant seedlings were fixed (Figure 4) in

859 3.5% glutaraldehyde and subject to cell separation in 0.1M EDTA, pH9, prior to

860 observation in a differential interference contrast Nikon Optiphot-2 microscope.

861   Cells (n=13-18) of four independent cotyledons per genotype were observed,

862   with cell plan areas, chloroplast number and individual area calculated as

863   described (Loudya et al., 2020).

864

Analysis of root development

866   Seedlings were cultured *in vitro*, under the conditions described in Supplemental

867   Figure 1, images taken and root length quantified using ImageJ (ImageJ.net)

868   software.

869

Map-based cloning of *cue8*.

871   Two mapping populations were generated following a *cue8* x La-*er* cross. In one,

872   F2 mutant plants were selected (genotype *cue8/cue8*); in another, wild type (WT)

873   plants were selected, grown to maturity and their progeny individually scored to

874   identify plants without *cue8* progeny (genotype +/+). A third mutant mapping

875   population was generated following a *cue8* x Col-0 cross. 344, 557 and 619

876   plants were selected respectively (total 1520 plants) in the three mapping

877   populations. Plants were examined at polymorphic markers 541 and 692 (Col-0

878   population) or 576 and 613 (La-*er* populations). DNA was extracted from pools of

879   3-4 plants, was examined and, if a recombination event identified, individual

880   plants were retested to identify the recombinant. Other polymorphisms between

881   Col-0 and La-*er* (TAIR, www.arabidopsis.org) were developed as polymorphic

882   markers by designing flanking primers for PCR amplification and differential

883   enzyme digestion (Supplemental Table 1), and screening Col-0, La-*er* and

884   pOCA108 genomic DNA. pOCA108 sequence was more frequently found to be

885   polymorphic against La-*er* (13/20) than against Col-0 (7/20). Genes in the region

886   of interest were ruled out by isolation of KOs of the SALK collection following

887   genotyping with the respective forward, reverse and border primers (Alonso et

888   al., 2003) (Supplemental Table 2). When no homozygous KO was identified

889   (AT5G22600, AT5G22640, AT5G22650, AT5G22660, AT5G22670, AT5G22680,

890   AT5G22710, AT5G22730), primer pairs were designed covering the full open

891   reading frame, and amplicons obtained using *cue8* genomic DNA template

892   submitted for Sanger sequencing (DNASeq, Medical Sciences Institute,

893   University of Dundee, UK). When polymorphisms against the TAIR sequence

894   occurred, amplicons for the pOCA108 WT were also sequenced (AT5G22640,

895   AT5G22650, AT5G22660, AT5G22670, AT5G22710, AT5G22730).

896

897   **Vector construction and complementation.**

898   A Transformation-competent Artificial Chromosome (TAC (Liu et al., 2000), JatY-

899   57L07, containing the genomic region covering genes AT5G22640 to

900   AT5G22740, was obtained as an *E. coli* stab culture from the John Innes Centre

901   (Norwich, UK). The TAC was introduced into *Agrobacterium* strain GV3101 by

902   electroporation, followed by transformation of Arabidopsis *cue8* using the floral

903   dip method (Clough and Bent, 1998). Selection of transformants utilised

904   resistance to BASTA (Glufosinate), sprayed at 150mg/l as a mist every 3 days.

905   Diagnostic PCR used the primers pYLTAC17-F (AATCCTGTTGCCCDCCTTG) in

906   the vector, and 57L07-FOR-R (GTCTGAGCCAGAGCCAGAGCTTGAGG) in the

907   insert, and produced a 607 bp amplicon. A separate TAC, JatY-76P13, covering

908   a broader region, was employed in the same way but generated no

909   transformants.

910   To produce a full-length WT cDNA, RNA was isolated (RNeasy kit, Qiagen,

911   Manchester, UK) from pOCA108 plants, cDNA synthesised (AMV Reverse

912   Transcriptase kit, Promega, Southampton, UK) and amplified with primers

913   CUE8cDNA-F (CACCATGGCTAACGAAGAACTCAC) and CUE8cDNA-STOP-R

914   (AGAGACTCAAGACACAGCAGGA) using BIO-X-ACT Long DNA polymerase

915   (Bioline, London, UK). The 2622 bp product was directionally cloned by ligation

916   into the pENTR/D-TOPO vector (Invitrogen/Thermo Fisher Scientific, Hemel

917   Hempstead, UK). Digestion with EcoRV and NotI generated 2742 and 2435

918   bands, confirming the cloning of the full-length cDNA, and that with EcoRI and

919   EcoRV generated 591 and 4586 bp bands, confirming the forward orientation.

920   Sequencing confirmed the absence of errors. The TOPO vector insert was

921   cloned into pB7WG2 vector (Karimi et al., 2002) using Gateway recombination, to

922   produce the pB7WG2/CUE8c construct. The pB7WG2 vector includes an

923   upstream 35S promoter. Sequencing confirmed the correct orientation and

924   absence of errors. Transformation of pB7WG2/CUE8c used the floral dip method.

925   Transformants were selected using BASTA. Primers cDNAgate-F

926   (TGCCCAGCTATCTGTCACTTC) in the vector, and cDNAgate-R

927   (CTTCCAACGTTCTGGGTCTC) in the *CUE8* sequence, generated a diagnostic

928   808 bp amplicon.

929

930   ***In silico* structure and expression analysis.**

931   Domain structure of the polypeptide sequence was analysed at

932   https://www.ebi.ac.uk/interpro/protein/UniProt/. Three-dimensional predicted

933   structure was obtained at https://alphafold.ebi.ac.uk/.

934   Expression of *CUE8/TIC100/EMB1211* in the Arabidopsis GeneAtlas data

935   (Schmid et al., 2005), available at

936   http://jsp.weigelworld.org/AtGenExpress/resources/, was compared with that of a

937   typical photosynthetic protein, *LHCB2* (AT2G05100) and a housekeeping plastid

938   import component, *TOC34* (AT5G05000). Gene expression correlators in relation

939   to development, AtGenExpress tissue compendium (Schmid et al., 2005) were

940   identified using the BioArray Resource (Toufighi et al., 2005) available at

941   http://bar.utoronto.ca/. Coexpressors were also identified using ATTD-II

942   (Obayashi et al., 2018).

943

944   **Chloroplast protein import assays and protein immunoblots.**

945   Chloroplasts were isolated from seedlings (Figure 3 and Figure 6) grown *in vitro*

946   to equivalent stages of cotyledons and first leaf pair, for approximately 13 days

947   (WT) and 17 days (mutants). Chloroplasts were isolated, examined by phase-

948   contrast microscopy to confirm integrity, and their density quantified. Isolation

949   and import assays using equal numbers of chloroplasts and the RBCS and

950   RPL11 radiolabelled pre-proteins were carried out as previously described (Kubis

951   et al., 2003). The fraction of pre-protein imported, obtained by quantifying on the

952   same import product gel, depended on assay but was at least 10%. Extracts of

953   total chloroplast protein were prepared and equal amounts of protein of WT and

954   mutant were fractionated and subject to immunoblot using specific antibodies, as

955   described (Kikuchi et al., 2013). Protein samples were denatured at 100 °C for 5

956   minutes except for the TIC214 (37 °C for 30 minutes) as described (Kikuchi et al.,

957   2013). Antibody dilutions are given in the Supplemental Table 5. Quantitation of

958   bands was carried out as described (Kubis et al., 2003) or using ImageJ

959   software.

960

961   **RNA extraction and quantitative real-time RT-PCR analysis.**

962   Total RNA was extracted from *in vitro*-grown (under continuous light) 5-day-old

963   wild type and 6-day-old *tic100^{cue8}* seedlings. Age differences other than 24h

964   could have resulted in spurious circadian effects. Nucleic acid extraction and

965   quantitation, cDNA synthesis, real time-PCR amplifications, assessment of

966   product quality and quantitation of expression in the mutant relative to that in the

967   pOCA108 wild type was carried out as previously described (Loudya et al.,

968   2020). Primer pairs for qRT-PCR are listed in Supplemental Table 6.

969

970   **Mutagenesis and isolation of *soh1*.**

971   The *tic100^{cue8}* seeds (over 5,000) were mutagenized using 50 mM ethyl

972   methanesulfonate for 4 hrs. About 5,000 healthy M1 *tic100^{cue8}* plants (carrying

973   heterozygous mutations) were grown as 50 pools. A putative suppressor in the

974   M2 population from pool 18 was isolated several times and found to have a

975   dramatic phenotype after 2 weeks on soil, which was confirmed by genotyping for

976   the *tic100^{cue8}* mutation. The protochlorophyllide and chlorophyll content in its M3

977   progeny seedlings further showed a clear suppression of *tic100^{cue8}*. Genetic

978   analysis of a backcross led to the conclusion of a semi-dominant suppressor

979   mutation. Pair-wise crosses of these suppressors from pool 18 showed them to

980   be allelic.

981

Protochlorophyllide and chlorophyll content.

Pigments were extracted in dimethyl formamide and quantitation was carried out

by spectrophotometry or spectrofluorimetry as previously described (López-Juez

et al., 1998; Vinti et al., 2005).

986

Mapping by sequencing of the *soh1* mutation.

The *soh1* mutation was identified by short-read mapping of a DNA pool from 150

backcrossed BC1F2 (see Supplemental Figure 5) recombinant *tic100^cue8^*

phenotypes (F), as well as 100 unmutagenised *tic100^cue8^* wild types (P1) and 100

homozygous *soh1* (P2) parents. Sequencing was carried out at the Oxford

Genomics Centre, Wellcome Trust Centre for Human Genetics

(http://www.well.ox.ac.uk/ogc/) and mapping-by-sequencing was performed using

the SHOREmap analysis package

(http://bioinfo.mpipz.mpg.de/shoremap/guide.html). To narrow the region, filters

were set for quality reads (>100) and indels were included to make sure the

polymorphisms of Bensheim were not considered as causal mutations. To

identify the semi-dominant mutation a mapping strategy was designed to first

compare the polymorphisms in the *tic100^cue8^ soh1* parent (P2, test) caused by

mutagenesis and that are absent in the *tic100^cue8^* parent (P1, reference) which

gave list A. Secondly, the polymorphisms (induced mutations) in the backcrossed

F2 *tic100^cue8^* population which are absent in P1 resulted in list B. In the last step,

list A was used as a test and list B as a reference to find out the EMS-induced

true SNPs.

1005

Gene cloning and generation of transgenic plants.

Gene cloning was performed using Gateway® Technology (Invitrogen). The

primers used for the generation of transgenic plants and transient assays are

listed in the Supplemental Table 7. The full coding sequences (CDSs) of

*tic100^soh1^* and *tic100^cue8^* genes were PCR amplified from the cDNA of the

1011 respective Arabidopsis genotypes (Bensheim). The CDSs from entry and

1012 destination vectors were confirmed by sequencing (Eurofins Genomics,

1013 Constance, Germany) and transformed into the $tic100^{cue8}$ mutant using

1014 *Agrobacterium*-mediated transformation (floral dipping). At least 10 T1 plants

1015 resistant on BASTA plates were genotyped in each case (35S:$tic100^{soh1}$and

1016 35S:$tic100^{cue8}$) and confirmed to carry the transgene.

1017

1018 **Subcellular localisation of TIC100 fluorescent protein fusions.**

1019 To study the protein localization using YFP fluorescence, the CDSs of *TIC100,*

1020 $tic100^{cue8}$ and $tic100^{soh1}$ genes were PCR-amplified without the stop codon from

1021 the cDNA of their Arabidopsis parent (Bensheim genotype). The CDSs were

1022 introduced into the entry vector, sequenced and later subcloned into the plant

1023 expression vector p2GWY7 carrying a C-terminal YFP tag (Karimi et al., 2005).

1024 Protoplast isolation and transfection assays were carried out as described

1025 previously (Wu et al., 2009; Ling et al., 2012). Plasmid DNA (5 µg) was

1026 transfected to 10^5 protoplasts (0.1 ml of protoplast suspension) isolated from

1027 healthy leaves of Arabidopsis Columbia.

1028 The YFP fluorescence images were captured using a Leica TCS SP5 microscope

1029 as described previously (Ling et al., 2019). Images shown represent results of at

1030 least two independent experiments (at least 40 protoplasts per genotype)

1031 showing the same result.

1032

1033 **Lincomycin treatment and associated immunoblot.**

1034 Seeds were plated and seedlings grown *in vitro* as indicated above without

1035 lincomycin. For lincomycin treatment, seeds were plated on a sterile, fine nylon

1036 mesh overlaying MS medium with 1% sucrose for 36 hours, at which time the

1037 mesh with germinating seeds was transferred to new medium containing in

1038 addition 0.5 mM lincomycin, where they continued to grow. Seedlings were

1039 harvested for transcripts' analysis at comparable developmental stages: 5 days

1040 for wild type, 6 days for $tic100^{cue8}$ and $tic100^{soh1}$ and 7 for $tic100^{soh1}$ *gun1*, with

1041 two additional days for protein analysis in each case. Total protein extraction

1042 using a urea/acetone powders method, incubation with a primary antibody

1043 against FtsH2 (Var2) and secondary antibody detection were as described

1044 (Loudya et al., 2021).

1045

1046 **Quantitation of RNA editing.**

1047 Monitoring and quantitation of editing of two chloroplast mRNAs was carried out

1048 as previously described (Loudya et al., 2020).

1049

1050 **Statistical analyses.**

1051 Averages and standard errors of the mean are indicated. Regressions, Chi-

1052 squared, Student's t-tests (two-tailed) and ANOVA followed by Dunnett's tests

1053 were carried out in Microsoft Excel ®, with plug-ins from Real-Statistics.com, for

1054 data using the numbers of replicates indicated for each experiment. For

1055 morphological parameters, chloroplast quantitative data, chloroplast

1056 preparations, import assays, immunoblots and gene expression assays, the

1057 number of samples represent independent biological replicates.

1058

1059 **Supplemental Data.**

1060

1061 **Supplemental Figure 1.** Mutation of *CUE8* delays root development, which can

1062 be partly but not fully rescued by growth on sucrose. Supports Figure 1.

1063 **Supplemental Figure 2.** Complementation of *cue8* by genomic DNA containing

1064 *TIC100.* Supports Figure 2.

1065 **Supplemental Figure 3.** Developmental expression of *TIC100*, in relation to that

1066 of a characteristic photosynthesis-associated and a characteristic plastid

1067 housekeeping protein nucleus-encoded gene. Supports Figures 2 and 6.

1068 **Supplemental Figure 4.** Chloroplasts of *tic100^{cue8}* exhibit reduction specifically

1069 in 1 MDa complex component proteins. Supports Figure 3.

Supplemental Figure 5. Semidominant phenotype of the *soh1* mutation, and the mapping strategy for gene identification. Supports Figure 5.

Supplemental Figure 6. Overexpression of *tic100^cue8* in the *tic100^cue8* mutant does not suppress the mutant phenotype. Supports Figure 5E.

Supplemental Figure 7. Localisation of the TIC100 protein, in its wild type, TIC100^cue8 and double-mutated TIC100^soh1 forms, to the cytoplasm and the chloroplast periphery of transformed, over-expressing intact protoplasts. Supports Figure 5F.

Supplemental Figure 8. Expression of *TIC/TOC* genes in *tic100^cue8 gun1* and *gun1* seedlings, measured relative to their expression in the wild type. Supports Figure 7.

Supplemental Table 1. List of polymorphic markers used for map-based cloning of *CUE8.* Supports Figure 2.

Supplemental Table 2. Analysis of the genomic region containing the *CUE8* gene, and strategies used to rule out alternatives. Supports Figure 2.

Supplemental Table 3. Polymorphisms in the *TIC100* sequence between the different genotypes and mutants. Supports Figure 2.

Supplemental Table 4. Primers used for genotyping the point mutants by dCAPS /CAPS.

Supplemental Table 5. Antibody dilutions used in immunoblotting.

Supplemental Table 6. List of primers used for quantitative real-time RT-PCR.

Supplemental Table 7. Primers used for gene cloning and transgenic approaches.

Supplemental Datasets 1 and 2. Developmental expression co-regulators of *CUE8* identified using Arabidopsis Gene Atlas data, and expression co-regulators according to ATTED-II.

Acknowledgments

1112

1113   **Author contributions:** NL, DM, JB, RPJ and ELJ designed the research. DM

1114   with assistance of ELJ cloned the *CUE8* gene. NL isolated *soh1* and cloned the

1115   gene with assistance from SMA. NL and JB performed *in vitro* import assays and

1116   associated immunoblot experiments. NL performed all microscopy analysis, gene

1117   expression quantitation, cloning of fusion proteins, subcellular localisation,

1118   lincomycin-associated immunoblot and RNA editing assays. NL and ELJ

1119   performed genetics, coexpression and protein folding analyses. NL, RPJ and ELJ

1120   wrote the manuscript. PFD, RPJ and ELJ supervised the project.

1121
1122

Parsed Citations

Alonso, J.M., Stepanova, A.N., Leisse, T.J., Kim, C.J., Chen, H.M., Shinn, P., Stevenson, D.K., Zimmerman, J., Barajas, P., Cheuk, R., Gadrinab, C., Heller, C., Jeske, A, Koesema, E., Meyers, C.C., Parker, H., Prednis, L., Ansari, Y., Choy, N., Deen, H., Geralt, M., Hazari, N., Hom, E., Karnes, M., Mulholland, C., Ndubaku, R., Schmidt, I., Guzman, P., Aguilar-Henonin, L., Schmid, M., Weigel, D., Carter, D.E., Marchand, T., Risseeuw, E., Brogden, D., Zeko, A, Crosby, W.L., Berry, C.C., and Ecker, J.R. (2003). Genome-wide Insertional mutagenesis of Arabidopsis thaliana. Science 301, 653-657.
Google Scholar: Author Only Title Only Author and Title

Arsovski, A.A., Galstyan, A, Guseman, J.M., and Nemhauser, J.L. (2012). Photomorphogenesis. The Arabidopsis book / American Society of Plant Biologists 10, e0147.
Google Scholar: Author Only Title Only Author and Title

Bolter, B., and Soll, J. (2016). Once upon a Time - Chloroplast Protein Import Research from Infancy to Future Challenges. Mol Plant 9, 798-812.
Google Scholar: Author Only Title Only Author and Title

Bolter, B., and Soll, J. (2017). Ycf1/Tic214 Is Not Essential for the Accumulation of Plastid Proteins. Mol Plant 10, 219-221.
Google Scholar: Author Only Title Only Author and Title

Borner, T., Aleynikova, A.Y., Zubo, Y.O., and Kusnetsov, V.V. (2015). Chloroplast RNA polymerases: Role in chloroplast biogenesis. Bba-Bioenergetics 1847, 761-769.
Google Scholar: Author Only Title Only Author and Title

Cackett, L., Luginbuehl, L.H., Schreier, T.B., Lopez-Juez, E., and Hibberd, J.M. (2021). Chloroplast development in green plant tissues: the interplay between light, hormone, and transcriptional regulation. New Phytol.
Google Scholar: Author Only Title Only Author and Title

Chen, L.j., and Li, H.m. (2017). Stable megadalton TOC–TIC supercomplexes as major mediators of protein import into chloroplasts. The Plant Journal 92, 178-188.
Google Scholar: Author Only Title Only Author and Title

Chen, X.J., Smith, M.D., Fitzpatrick, L., and Schnell, D.J. (2002). In vivo analysis of the role of atTic20 in protein import into chloroplasts. Plant Cell 14, 641-654.
Google Scholar: Author Only Title Only Author and Title

Chotewutmontri, P., and Barkan, A (2016). Dynamics of Chloroplast Translation during Chloroplast Differentiation in Maize. Plos Genet 12.
Google Scholar: Author Only Title Only Author and Title

Chu, C.C., Swamy, K., and Li, H.M. (2020). Tissue-Specific Regulation of Plastid Protein Import via Transit-Peptide Motifs. Plant Cell 32, 1204-1217.
Google Scholar: Author Only Title Only Author and Title

Clough, S.J., and Bent, A.F. (1998). Floral dip: a simplified method for Agrobacterium-mediated transformation of Arabidopsis thaliana. Plant J 16, 735-743.
Google Scholar: Author Only Title Only Author and Title

Dahlin, C., and Cline, K. (1991). Developmental regulation of the plastid protein import apparatus. The Plant Cell 3, 1131-1140.
Google Scholar: Author Only Title Only Author and Title

de Vries, J., Sousa, F.L., Bolter, B., Soll, J., and Gould, S.B. (2015). Ycf1: A Green Tic? Plant Cell 27, 1827-1833.
Google Scholar: Author Only Title Only Author and Title

Demarsy, E., Lakshmanan, A.M., and Kessler, F. (2014). Border control: selectivity of chloroplast protein import and regulation at the TOC-complex. Frontiers in plant science 5, 483.
Google Scholar: Author Only Title Only Author and Title

Haswell, E.S., and Meyerowitz, E.M. (2006). MscS-like proteins control plastid size and shape in Arabidopsis thaliana. Curr Biol 16, 1-11.
Google Scholar: Author Only Title Only Author and Title

Heins, L., Mehrle, A, Hemmler, R., Wagner, R., Kuchler, M., Hormann, F., Sveshnikov, D., and Soll, J. (2002). The preprotein conducting channel at the inner envelope membrane of plastids. EMBO Journal 21, 2616-2625.
Google Scholar: Author Only Title Only Author and Title

Inaba, T., Li, M., Alvarez-Huerta, M., Kessler, F., and Schnell, D.J. (2003). atTic110 functions as a scaffold for coordinating the stromal events of protein import into chloroplasts. Journal of Biological Chemistry 278, 38617-38627.
Google Scholar: Author Only Title Only Author and Title

Ivanova, Y., Smith, M.D., Chen, K., and Schnell, D.J. (2004). Members of the Toc159 import receptor family represent distinct pathways for protein targeting to plastids. Molecular Biology of the Cell 15, 3379-3392.
Google Scholar: Author Only Title Only Author and Title

Jarvis, P. (2008). Targeting of nucleus-encoded proteins to chloroplasts in plants. New Phytol 179, 257-285.
Google Scholar: Author Only Title Only Author and Title

Jarvis, P., and López-Juez, E. (2013). Biogenesis and homeostasis of chloroplasts and other plastids. Nature reviews. Molecular cell biology 14, 787-802.
Google Scholar: Author Only Title Only Author and Title

Jumper, J., Evans, R., Pritzel, A, Green, T., Figurnov, M., Ronneberger, O., Tunyasuvunakool, K., Bates, R., Zidek, A, Potapenko, A, Bridgland, A, Meyer, C., Kohl, S.A.A, Ballard, A.J., Cowie, A, Romera-Paredes, B., Nikolov, S., Jain, R., Adler, J., Back, T., Petersen, S., Reiman, D., Clancy, E., Zielinski, M., Steinegger, M., Pacholska, M., Berghammer, T., Bodenstein, S., Silver, D., Vinyals, O., Senior, A.W., Kavukcuoglu, K., Kohli, P., and Hassabis, D. (2021). Highly accurate protein structure prediction with AlphaFold. Nature.
Google Scholar: Author Only Title Only Author and Title

Kakizaki, T., Yazu, F., Nakayama, K., Ito-Inaba, Y., and Inaba, T. (2012). Plastid signalling under multiple conditions is accompanied by a common defect in RNA editing in plastids. J Exp Bot 63, 251-260.
Google Scholar: Author Only Title Only Author and Title

Karimi, M., Inze, D., and Depicker, A. (2002). GATEWAY vectors for Agrobacterium-mediated plant transformation. Trends Plant Sci 7, 193-195.
Google Scholar: Author Only Title Only Author and Title

Karimi, M., De Meyer, B., and Hilson, P. (2005). Modular cloning in plant cells. Trends Plant Sci 10, 103-105.
Google Scholar: Author Only Title Only Author and Title

Kasmati, A.R., Topel, M., Patel, R., Murtaza, G., and Jarvis, P. (2011). Molecular and genetic analyses of Tic20 homologues in Arabidopsis thaliana chloroplasts. Plant J 66, 877-889.
Google Scholar: Author Only Title Only Author and Title

Kessler, F., and Blobel, G. (1996). Interaction of the protein import and folding machineries in the chloroplast. P Natl Acad Sci USA 93, 7684-7689.
Google Scholar: Author Only Title Only Author and Title

Kikuchi, S., Bedard, J., Hirano, M., Hirabayashi, Y., Oishi, M., Imai, M., Takase, M., Ide, T., and Nakai, M. (2013). Uncovering the protein translocon at the chloroplast inner envelope membrane. Science 339, 571-574.
Google Scholar: Author Only Title Only Author and Title

Kikuchi, S., Asakura, Y., Imai, M., Nakahira, Y., Kotani, Y., Hashiguchi, Y., Nakai, Y., Takafuji, K., Bedard, J., Hirabayashi-Ishioka, Y., Mori, H., Shiina, T., and Nakai, M. (2018). A Ycf2-FtsHi Heteromeric AAA-ATPase Complex Is Required for Chloroplast Protein Import. Plant Cell 30, 2677-2703.
Google Scholar: Author Only Title Only Author and Title

Klepikova, A.V., Kasianov, A.S., Gerasimov, E.S., Logacheva, M.D., and Penin, A.A. (2016). A high resolution map of the Arabidopsis thaliana developmental transcriptome based on RNA-seq profiling. Plant J 88, 1058-1070.
Google Scholar: Author Only Title Only Author and Title

Kohler, D., Helm, S., Agne, B., and Baginsky, S. (2016). Importance of Translocon Subunit Tic56 for rRNA Processing and Chloroplast Ribosome Assembly. Plant Physiol 172, 2429-2444.
Google Scholar: Author Only Title Only Author and Title

Kohler, D., Montandon, C., Hause, G., Majovsky, P., Kessler, F., Baginsky, S., and Agne, B. (2015). Characterization of Chloroplast Protein Import without Tic56, a Component of the 1-Megadalton Translocon at the Inner Envelope Membrane of Chloroplasts. Plant Physiol 167, 972-990.
Google Scholar: Author Only Title Only Author and Title

Koussevitzky, S., Nott, A, Mockler, T.C., Hong, F., Sachetto-Martins, G., Surpin, M., Lim, I.J., Mittler, R., and Chory, J. (2007). Signals from chloroplasts converge to regulate nuclear gene expression. Science 316, 715-719.
Google Scholar: Author Only Title Only Author and Title

Kovacs-Bogdan, E., Benz, J.P., Soll, J., and Bolter, B. (2011). Tic20 forms a channel independent of Tic110 in chloroplasts. Bmc Plant Biol 11, 133.
Google Scholar: Author Only Title Only Author and Title

Kubis, S., Baldwin, A, Patel, R., Razzaq, A, Dupree, P., Lilley, K., Kurth, J., Leister, D., and Jarvis, P. (2003). The Arabidopsis ppi1 mutant is specifically defective in the expression, chloroplast import, and accumulation of photosynthetic proteins. Plant Cell 15, 1859-1871.

Google Scholar: Author Only Title Only Author and Title

Kubis, S., Patel, R., Combe, J., Bedard, J., Kovacheva, S., Lilley, K., Biehl, A, Leister, D., Rios, G., Koncz, C., and Jarvis, P. (2004). Functional specialization amongst the Arabidopsis Toc159 family of chloroplast protein import receptors. Plant Cell 16, 2059-2077.
  Google Scholar: Author Only Title Only Author and Title

Li, H.M., Culligan, K., Dixon, R.A., and Chory, J. (1995). Cue1 - a Mesophyll Cell-Specific Positive Regulator of Light-Controlled Gene-Expression in Arabidopsis. Plant Cell 7, 1599-1610.
  Google Scholar: Author Only Title Only Author and Title

Liang, Q.J., Lu, X.D., Jiang, L., Wang, C.Y., Fan, Y.L., and Zhang, C.Y. (2010). EMB1211 is required for normal embryo development and influences chloroplast biogenesis in Arabidopsis. Physiol Plantarum 140, 380-394.
  Google Scholar: Author Only Title Only Author and Title

Ling, Q., Huang, W., Baldwin, A, and Jarvis, P. (2012). Chloroplast biogenesis is regulated by direct action of the ubiquitin-proteasome system. Science 338, 655-659.
  Google Scholar: Author Only Title Only Author and Title

Ling, Q., Broad, W., Trosch, R., Topel, M., Demiral Sert, T., Lymperopoulos, P., Baldwin, A, and Jarvis, R.P. (2019). Ubiquitin-dependent chloroplast-associated protein degradation in plants. Science 363, 836-848.
  Google Scholar: Author Only Title Only Author and Title

Liu, Y.G., Nagaki, K., Fujita, M., Kawaura, K., Uozumi, M., and Ogihara, Y. (2000). Development of an efficient maintenance and screening system for large-insert genomic DNA libraries of hexaploid wheat in a transformation-competent artificial chromosome (TAC) vector. Plant J 23, 687-695.
  Google Scholar: Author Only Title Only Author and Title

López-Juez, E., Jarvis, R.P., Takeuchi, A, Page, A.M., and Chory, J. (1998). New Arabidopsis cue mutants suggest a close connection between plastid- and phytochrome regulation of nuclear gene expression. Plant Physiol 118, 803-815.
  Google Scholar: Author Only Title Only Author and Title

Loudya, N., Okunola, T., He, J., Jarvis, P., and López-Juez, E. (2020). Retrograde signalling in a virescent mutant triggers an anterograde delay of chloroplast biogenesis that requires GUN1 and is essential for survival. Philosophical transactions of the Royal Society of London. Series B, Biological sciences 375, 20190400.
  Google Scholar: Author Only Title Only Author and Title

Loudya, N., Mishra, P., Takahagi, K., Uehara-Yamaguchi, Y., Inoue, K., Bogre, L., Mochida, K., and Lopez-Juez, E. (2021). Cellular and transcriptomic analyses reveal two-staged chloroplast biogenesis underpinning photosynthesis build-up in the wheat leaf. Genome Biol 22.
  Google Scholar: Author Only Title Only Author and Title

Lubeck, J., Soll, J., Akita, M., Nielsen, E., and Keegstra, K. (1996). Topology of IEP110, a component of the chloroplastic protein import machinery present in the inner envelope membrane. EMBO Journal 15, 4230-4238.
  Google Scholar: Author Only Title Only Author and Title

Nakai, M. (2015a). The TIC complex uncovered: The alternative view on the molecular mechanism of protein translocation across the inner envelope membrane of chloroplasts. Bba-Bioenergetics 1847, 957-967.
  Google Scholar: Author Only Title Only Author and Title

Nakai, M. (2015b). YCF1: A Green TIC: Response to the de Vries et al. Commentary. Plant Cell 27, 1834-1838.
  Google Scholar: Author Only Title Only Author and Title

Nakai, M. (2018). New Perspectives on Chloroplast Protein Import. Plant Cell Physiol 59, 1111-1119.
  Google Scholar: Author Only Title Only Author and Title

Nakai, M. (2020). Reply: The Revised Model for Chloroplast Protein Import. Plant Cell 32, 543-546.
  Google Scholar: Author Only Title Only Author and Title

Obayashi, T., Aoki, Y., Tadaka, S., Kagaya, Y., and Kinoshita, K. (2018). ATTED-II in 2018: A Plant Coexpression Database Based on Investigation of the Statistical Property of the Mutual Rank Index. Plant Cell Physiol 59, 440.
  Google Scholar: Author Only Title Only Author and Title

Ramundo, S., Asakura, Y., Salome, P.A, Strenkert, D., Boone, M., Mackinder, L.C.M., Takafuji, K., Dinc, E., Rahire, M., Crevecoeur, M., Magneschi, L., Schaad, O., Hippler, M., Jonikas, M.C., Merchant, S., Nakai, M., Rochaix, J.D., and Walter, P. (2020). Coexpressed subunits of dual genetic origin define a conserved supercomplex mediating essential protein import into chloroplasts. P Natl Acad Sci USA 117, 32739-32749.
  Google Scholar: Author Only Title Only Author and Title

Richardson, L.G.L., and Schnell, D.J. (2020). Origins, function, and regulation of the TOC-TIC general protein import machinery of plastids. J Exp Bot 71, 1226-1238.
  Google Scholar: Author Only Title Only Author and Title

Richardson, L.G.L., Small, E.L., Inoue, H., and Schnell, D.J. (2018). Molecular Topology of the Transit Peptide during Chloroplast Protein Import. Plant Cell 30, 1789-1806.
Google Scholar: Author Only Title Only Author and Title

Schafer, P., Helm, S., Kohler, D., Agne, B., and Baginsky, S. (2019). Consequences of impaired 1-MDa TIC complex assembly for the abundance and composition of chloroplast high-molecular mass protein complexes. PLoS One 14, e0213364.
Google Scholar: Author Only Title Only Author and Title

Schmid, M., Davison, T.S., Henz, S.R., Pape, U.J., Demar, M., Vingron, M., Scholkopf, B., Weigel, D., and Lohmann, J.U. (2005). A gene expression map of Arabidopsis thaliana development. Nat Genet 37, 501-506.
Google Scholar: Author Only Title Only Author and Title

Schneeberger, K., Ossowski, S., Lanz, C., Juul, T., Petersen, A.H., Nielsen, K.L., Jørgensen, J.-E., Weigel, D., and Andersen, S.U.J.N.m. (2009). SHOREmap: simultaneous mapping and mutation identification by deep sequencing. Nat Methods 6, 550.
Google Scholar: Author Only Title Only Author and Title

Sjuts, I., Soll, J., and Bolter, B. (2017). Import of Soluble Proteins into Chloroplasts and Potential Regulatory Mechanisms. Frontiers in plant science 8, 168.
Google Scholar: Author Only Title Only Author and Title

Susek, R.E., Ausubel, F.M., and Chory, J.J.C. (1993). Signal transduction mutants of Arabidopsis uncouple nuclear CAB and RBCS gene expression from chloroplast development. Cell 74, 787-799.
Google Scholar: Author Only Title Only Author and Title

Tadini, L., Pesaresi, P., Kleine, T., Rossi, F., Guljamow, A., Sommer, F., Mühlhaus, T., Schroda, M., Masiero, S., and Pribil, M.J.P.p. (2016). GUN1 controls accumulation of the plastid ribosomal protein S1 at the protein level and interacts with proteins involved in plastid protein homeostasis. Plant Physiol, pp. 02033.02015.
Google Scholar: Author Only Title Only Author and Title

Tadini, L., Peracchio, C., Trotta, A., Colombo, M., Mancini, I., Jeran, N., Costa, A., Faoro, F., Marsoni, M., Vannini, C., Aro, E.M., and Pesaresi, P. (2020). GUN1 influences the accumulation of NEP-dependent transcripts and chloroplast protein import in Arabidopsis cotyledons upon perturbation of chloroplast protein homeostasis. Plant J 101, 1198-1220.
Google Scholar: Author Only Title Only Author and Title

Takeshima, H., Komazaki, S., Nishi, M., Iino, M., and Kangawa, K. (2000). Junctophilins: a novel family of junctional membrane complex proteins. Mol Cell 6, 11-22.
Google Scholar: Author Only Title Only Author and Title

Teng, Y.S., Chan, P.T., and Li, H.M. (2012). Differential age-dependent import regulation by signal peptides. PLoS Biol 10, e1001416.
Google Scholar: Author Only Title Only Author and Title

Toufighi, K., Brady, S.M., Austin, R., Ly, E., and Provart, N.J. (2005). The Botany Array Resource: e-Northerns, Expression Angling, and Promoter analyses. Plant J 43, 153-163.
Google Scholar: Author Only Title Only Author and Title

Tsai, J.Y., Chu, C.C., Yeh, Y.H., Chen, L.J., Li, H.M., and Hsiao, C.D. (2013). Structural characterizations of the chloroplast translocon protein Tic110. Plant J 75, 847-857.
Google Scholar: Author Only Title Only Author and Title

Vinti, G., Fourrier, N., Bowyer, J.R., and López-Juez, E. (2005). Arabidopsis cue mutants with defective plastids are impaired primarily in the photocontrol of expression of photosynthesis-associated nuclear genes. Plant Mol Biol 57, 343-357.
Google Scholar: Author Only Title Only Author and Title

Vojta, A., Alavi, M., Becker, T., Hormann, F., Kuchler, M., Soll, J., Thomson, R., and Schleiff, E. (2004). The protein translocon of the plastid envelopes. J Biol Chem 279, 21401-21405.
Google Scholar: Author Only Title Only Author and Title

Wu, F.H., Shen, S.C., Lee, L.Y., Lee, S.H., Chan, M.T., and Lin, C.S. (2009). Tape-Arabidopsis Sandwich - a simpler Arabidopsis protoplast isolation method. Plant Methods 5, 16.
Google Scholar: Author Only Title Only Author and Title

Wu, G.Z., Meyer, E.H., Richter, A.S., Schuster, M., Ling, Q., Schottler, M.A., Walther, D., Zoschke, R., Grimm, B., Jarvis, R.P., and Bock, R. (2019). Control of retrograde signalling by protein import and cytosolic folding stress. Nat Plants 5, 525-538.
Google Scholar: Author Only Title Only Author and Title